catalysts

MDPI

Review

Recent Development in Non-Metal-Doped Titanium Dioxide Photocatalysts for Different Dyes Degradation and the Study of Their Strategic Factors: A Review

Parveen Akhter [1,*], Abdullah Arshad [1], Aimon Saleem [1] and Murid Hussain [2,*]

[1] Department of Chemistry, The University of Lahore, 1-Km Defence Road, Off Raiwind Road, Lahore 54000, Pakistan
[2] Department of Chemical Engineering, COMSATS University Islamabad, Lahore Campus, Defence Road, Off Raiwind Road, Lahore 54000, Pakistan
* Correspondence: parveen.akhter@chem.uol.edu.pk (P.A.); drmhussain@cuilahore.edu.pk (M.H.)

Abstract: Semiconductor titanium dioxide in its basic form or doped with metals and non-metals is being extensively used in wastewater treatment by photocatalysis due to its versatile nature. Other numerous characteristics including being environmentally friendly, non-pernicious, economical, multi-phase, highly hydrophilic, versatile physio-chemical features, chemical stability, suitable band gap, and corrosion-resistance, along with its low price make TiO_2 the best candidate in the field of photocatalysis. Commercially, semiconductor and synthesized photocatalysts—which have been investigated for the last few decades owing to their wide band gap—and the doping of titania with p-block elements (non-metals) such as oxygen, sulfur, nitrogen, boron, carbon, phosphorus, and iodine enhances their photocatalytic efficiency under visible-light irradiation. This is because non-metals have a strong oxidizing ability. The key focus of this review is to discuss the various factors affecting the photocatalytic activity of non-metal-doped titania by decreasing its band gap. The working parameters discussed are the effect of pH, dyes concentration, photocatalyst's size and structure, pollutants concentration and types, the surface area of photocatalysts, the effect of light intensity and irradiation time, catalyst loading, the effect of temperature, and doping impact, etc. The mechanism of the photocatalytic action of several non-metallic dopants of titanium dioxide and composites is a promising approach for the exploration of photocatalysis activity. The various selected synthesis methods for non-metallic-doped TiO_2 have been reviewed in this study. Similarly, the effect of various conditions on the doping mode has been summarized in relation to several sorts of modified TiO_2.

Keywords: dyes degradation; non-metal-doped titania; photocatalysis; parameters; wastewater treatment

Citation: Akhter, P.; Arshad, A.; Saleem, A.; Hussain, M. Recent Development in Non-Metal-Doped Titanium Dioxide Photocatalysts for Different Dyes Degradation and the Study of Their Strategic Factors: A Review. *Catalysts* **2022**, *12*, 1331. https://doi.org/10.3390/catal12111331

Academic Editors: Rafael Borja, Gassan Hodaifa and Mha Albqmi

Received: 9 September 2022
Accepted: 26 October 2022
Published: 31 October 2022

1. Introduction

Water is one of the most precious and non-replaceable commodities of mankind. The per capita usage of water varies between countries and its demand includes domestic, industrial, and public, but here lies a problem of the misuse of water on a larger scale. Obviously, photocatalysis is the most fundamental technique for the degradation of organic pollutants and their conversion into valuable products, the removal of industrial effluents, and energy utilization [1,2]. Appropriate water supplies are the most important and key parameters for human consumption, industrial, agricultural, and domestic purposes. Generally, a wide range of natural and artificial contaminations has deleteriously affected the environment directly or indirectly, in which textile dye removal is of major concern [3–5]. However, ample research has been carried out on TiO_2 as a paramount photocatalyst for a variety of applications, such as the degradation of organic pollutants, hydrogen production from water splitting, the purification of air and water, self-cleansing surfaces, food cosmetics, the paint industry, etc. Titania is extensively employed in energy-associated

industries, specifically, in water splitting under visible-light irradiation [6]. However, different compounds have been used for the doping of TiO_2 with CdS [7]. SnO_2-doped TiO_2 [8–10], WO_3-doped TiO_2 [11], $ZrTiO_4$ [12–14], and are employed in the heterogeneous photocatalysis. Among these very endearing materials, non-metal-doped TiO_2 photocatalysts have gained significant attention due to their greater synergistic effect, which leads to the reduction in the band gap of titania from various metal-doped TiO_2 [14–16]. Many conventional techniques or pathways have been adopted for the wastewater treatment, but unfortunately, the problem remains unsolved. However, different measures such as adsorption, coagulation, flocculation, and oxidation have been employed to cast off dyes from wastewater. The most documented approaches for the removal of dyes from wastewater are precipitation, filtration, and electrochemical procedures. However, these methods also have disadvantages; moreover, some of them do not have the ability to break down the dye completely. Therefore, photocatalysis is now thought to be one of the best ways to remove dyes from contaminated water [17]. Additionally, to overcome this issue, the photocatalytic process of various dyes degradation has shown to be a more efficient, cost-effective, and convenient way to eliminate abundant contaminants and organic pollutants from water. This method has drawn the attention of researchers all over the world to the development of more effective techniques of wastewater treatment. For this mechanism, simple TiO_2, doped TiO_2, or composite of TiO_2 have been widely discussed in the literature [18–21]. Some modifications in titania can help in resolving the mistreatment of unadorned TiO_2. However, doping the TiO_2 would enhance the photocatalytic activity for a range of mechanisms, as well as reduce the band gap in TiO_2 materials [22]. The well-known polymorphs of TiO_2 are rutile, anatase, and brookite, which are naturally occurring. It has recently been demonstrated that photo-activity towards organic degradation depends on the phase composition and oxidizing agent; for example, when the performance of different crystalline forms was compared, it was discovered that rutile shows the highest photocatalytic activity with H_2O_2, whereas anatase shows the highest with O_2. A good photocatalyst should be photoactive, able to utilize visible and/or near UV light, and be biologically and chemically inert, photostable, inexpensive, and non-toxic. However, it was previously reported that the anatase phase of TiO_2 is more efficient owing to its excellent photocatalytic properties [19]. Rutile is stable and easy to fabricate in setting conditions, while brookite is metastable and the preparation is troublesome. Both rutile and anatase hold a tetragonal crystal structure with a band gap of approximately 3.0–3.2 eV, respectively [23]. Titania has many advantages; foremost important is its use as a photocatalyst, and it is innocuous and chemically stable, etc. However, it also has a few disadvantages, for instance, it has a higher energy gap around 3.2 eV, which is why its use is limited to UV light only. Moreover, it cannot be activated in visible light or sunlight; therefore, researchers have been working on other ways to use it. Few methods are being developed for this purpose; one of the methods is to dope non-metals or metals impurity, and the other is to introduce light-sensitive semiconductors such as WO_3 in order to enhance the photocatalytic activity of TiO_2 [24]. Below visible-light irradiation, metal doping enhances the performance of the doped TiO_2 by moving the absorption spectra into a low energy field. Metal doping, on the other hand, has significant disadvantages, including the thermal instability of doped TO_2, electron capture by metal centers, and the need for more expensive ion implants. Non-metallic doping increases the percentage of anatomical TiO_2, which slows down the formation of TiO_2 crystals and increases the specificity of titania [25]. The most important approach that is used widely is the sol-gel method, which produces high surface area TiO_2 by controlling the hydrolysis of titanium tetraisopropoxide (TTIP) [26]. Therefore, the re-integration of electron–hole pairs produced in the valence and conduction bands enhances the image performance of TiO_2 [27]. However, there is also provision for dye photosensitization and proper TiO_2 support with the help of an efficient TiO_2 modification method [28]. Likewise, mesoporous titania (mp-TiO_2) is considered the best due to its higher surface area, tunable pore-size distribution, and well-defined pore orientation [29]. Furthermore, nitrogen/fluorine (N/F) co-doped mp-TiO_2 has been shown

to exhibit improved visible-light adsorption and photoactivity [30]. TiO_2 graphene (Gr) porous microspheres were prepared by ultrasonic spray pyrolysis [31]. However, N/F co-doped mp-TiO_2 showed the best photocatalytic activity compared with single-element doping. The solvothermal method was adopted for the synthesis of N/F-mp-TiO_2, using urea as a nitrogen source and ammonium fluoride as a source for fluorine. There has been a great change in band gaps by the doping of TiO_2 with non-metals constituents, which are reported as F-TiO_2, N-TiO_2, B/N-TiO_2 [32], and C-N-S [33,34]. Moreover, thin-film TiO_2 with a different nano size is being extensively used for solar cell, design sensors, displays, automobiles rearview mirrors, and many other gas purification applications [35–37].

In this review, we have unfolded all the possible prospects and aspects of TiO_2 photocatalyst doped with non-metals for light sensitivity. By the end of the paper, almost all the precarious applications, challenges, and future recommendations will have been proposed.

2. Effect of Non-Metal Doping

Different approaches are investigated to prevent the recombination of electron–hole pairs that are photogenerated by undoped TiO_2. Doping adjusts the electronic assembly of TiO_2, which boosts it from the UV region toward visible spectra. The doping of titania with any species enhances their ability to confer the chemistry of that particular material; for example, a high degree of crystallinity is mainly due to a large surface area and a large crystal size, which ultimately increases the photocatalytic activity and decreases the charge separation of the photogenerated e^-/h^+ pair recombination [38,39]. Nevertheless, the doping or modification of TiO_2 using non-metal/anion has been carefully adopted to overcome the use of maximum energy, high photocatalytic activity, reduced time span of charge separation, and higher efficiency of TiO_2, and the effect of various parameters has been discussed here. Moreover, non-metallic dopants such as carbon (C) [40–42], nitrogen (N) [43–47], sulfur (S) [47,48], boron (B) [49,50], iodine (I) [51], N/F-doped TiO_2 [30,52], L-amino acids (C–N co-doped or C–N–S tri-doped)-TiO_2, C-N-TiO_2 /CNT composites, etc., have also been discussed (Table 1). The compatibility of (N) was investigated, and the improved photocatalytic performance and morphology of TiO_2 was observed [23], as well as its composites [15]. Furthermore, GO/TiO_2 nanocomposite showed an upgraded photocatalytic efficiency [53]. Attention is being diverted to the treatment of contaminated water with porous mineral composite materials. The growth of non-metallic spongy minerals has resulted in a high specific surface area, strong adsorption capabilities, and tailored chemical accumulation [54]. Montmorillonite-supported-TiO_2 (MMT/TiO_2) will solve the cohesion problem of TiO_2 particles. Contaminants can be adsorbed on the surface of nano TiO_2 to improve the probability of ion exchange and contact between the catalysts and contaminants deterioration rate. Therefore, a porous MMT/TiO_2 complex system can improve its photodecomposition efficiency by reducing the agglomeration and intensifying the photocatalytic response. The comparatively improved absorbance of the composite material in visible light is (390–780 nm); therefore, MMT/TiO_2 also improves the optical absorption capacity from 70 to 87%, instead of using TiO_2 individually [55].

Table 1. Summary of non-metal-doped TiO_2 photocatalyst under varied circumstances.

Year of Study	Type of Non-Metal Dopants	Synthesis Route/Method	Type of Dye	Characterization Techniques	Ref.
2017	C-TiO_2	Hydrothermal	Methylene blue, Rhodamine B, p nitrophenol	XRD, SEM, TEM, STEM, XPS, UV-vis	[56]
2019	C-TiO_2	Hydrothermal	Methylene blue	XRD, FTIR, N_2 adsorption-desorption isotherm, SEM, UV-vis	[57]
2020	C-TiO_2	Sol-gel	Methylene blue	EDX, UV-vis DRS analysis, SEM	[58]

Table 1. *Cont.*

Year of Study	Type of Non-Metal Dopants	Synthesis Route/Method	Type of Dye	Characterization Techniques	Ref.
2020	C-TiO_2 double-layer hollow microsphere	Hydrolysis of thermal expandable microsphere	Rhodamine B	XRD, FTIR, TGA, SEM, Raman N_2 adsorption-desorption isotherm, XPS, UV-vis	[59]
2021	Carbon-doped TiO_2 nanoparticles	Sol-gel	Methylene blue	XRD, TEM, XPS, DRS,138	[60]
2022	C-TiO_2 nanoflakes (C-TNFs)	Facile hydrothermal	Methylene blue	XRD, FTIR, SEM, UV-vis	[40]
2007	N-TiO_2	Microemulsion-hydrothermal	Rhodamine B	XRD, Raman, XPS, PL emission spectra	[61]
2010	N-TiO_2	Sol-gel/acidic media	Lindane	XRD, SEM, TEM, Raman, XPS, GC-MS	[62]
2015	N and C-co-doped porous TiO_2 nanofibers	Electrospinning and calcination	Methylene blue	XRD, FESEM, TEM, XPS, DRS,	[63]
2017	N-TiO_2	Solvothermal	Rhodamine B	XRD, SEM, TEM, BET, XPS, UV-vis	[64]
2020	TiN/N-doped TiO_2 composites	Sputtering process	Methylene blue	Raman, XPS, UV-vis	[65]
2020	C-N-TiO_2 composite fibers	Hydrolysis and calcination	Rhodamine B	XRD, SEM, TEM, FTIR, Raman, XPS, UV-vis	[66]
2021	N-TiO_2 nanotubes	Hydrothermal	Methyl orange	XRD, SEM, XPS, UV-vis	[67]
2009	S-TiO_2	Hydrothermal	Methylene orange	XRD, TEM	[68]
2015	S-TiO_2	Wet-impregnation method.	Humic acid Humic acid	EDX, SEM, EEM fluorescence	[69]
2016	(S–TiO_2), (N–S–TiO_2)	Sol-gel	Phenol and MB	BET, FESEM, FTIR, XPS, DRS	[70]
2011	S-TiO_2, N-S-TiO_2	Sol-gel	Methyl orange	XRD, TEM, UV-vis DRS	[71]
2021	NS/TiO_2	Sol-gel	Methylene blue, methyl red	XRD, BET, SEM, FTIR, Raman, UV-vis	[21]
	P/TiO_2	Hydrothermal/sol-gel			[72]
	Ag-P/TiO_2 nanofibers	One-pot electrospinning	Methylene blue	XRD, XPS, FE-SEM, TEM, UV-vis	[73]
2022	P/TiO_2/MWCNTs	Sol-gel	Methylene blue	XRD, FE-SEM, FTIR, UV-vis	[74]
2017	Si/TiO_2	Solvothermal	Methyl orange	XRD, SEM, EDS, BET, XPS	[75]

3. Treatment Opportunities for Dyes

Dyes have been a constant source of contamination for decades; textile and industrial dyes in the wastewater are one of the major contributors of toxic organic pollutants. The ever-increasing production of dyes is because of rapid industrialization; therefore, it is urgently necessary to focus on the proper treatment of these dyes [76]. In industries, most of the fabrication and processing operations excrete dyes in the wastewaters; the range of dyes varies from 2% to 50% from basic to reactive colorants, respectively. Therefore, the toxins produced are harmful for ground as well as surface water, as most of the compounds present in these hazardous dyes are non-biodegradable and likely to cause cancer [77]. Now, the primary concern is the sufficient treatment of these dyes; for their removal, various chemical and physical methods are being reported. Some of these methods are: ozonation [78], activated carbon [79], bio-degradation [80], and photocatalytic degradation using TiO_2, etc. [81]. The removal of dyes from contaminated water has been accomplished through biological processes that include microbiological or enzymatic decomposition and environmental degradation. Anaerobic conditions also contribute to the deterioration of the

azo bond, which leads to the removal of pigment, but also leads to an insufficient mineral formation of harmful and carcinogenic products. A variety of synthetic dyes have been extensively tested in recent years to develop a more promising method based on advanced oxidation processes (AOPs) that can release pollutants quickly and extensively. AOPs rely on the formation of highly active hydroxyl radicals ($OH^{\bullet}$), which can release any chemical present in a liquid matrix, usually with a reaction rate controlled by diffusion [82].

3.1. Types of Dyes

The method by which photo-degradation occurs is determined by the products generated, as these product molecules would be adsorbed on the surface of the semiconductor by modifying the layout of its electronic and active sites. In photo-catalytic degradation, it has been discovered that dyes with a positive charge (cationic) adsorb more on unaltered TiO_2 than dyes with a negative charge (anionic) [83]. Azo dyes (AzD) are attributed as the major (60–70%) class of synthetic dye stuff used in the textile, leather, oil, additives, and food industry, etc., and the resulting byproducts carry both the metal ion and the dyes. All the major classes of dyes are shown in Figure 1 and Table 2.

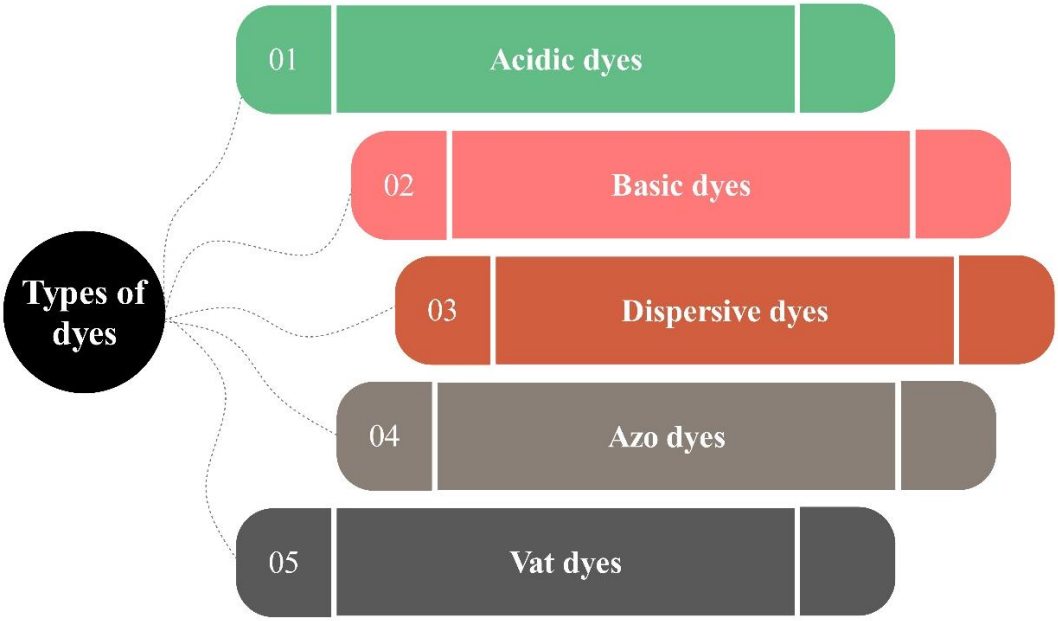

Figure 1. Major classes of dyes.

Table 2. Types and characteristics of Azo dyes [76].

Category of Dye	Features	Fiber	Pollutant	Dyes Fixation
Acidic	Water-soluble anionic compounds	Wool, nylon, cotton blends, acrylic, and protein fibers	Organic acids, unfixed dyes, color	80–93
Basic	Water-soluble, applied in weakly acidic dye baths, very bright dyes	Acrylic, cationic, polyester, nylon, cellulosic, and protein fibers	NA	97–98
Direct	Water-soluble, anionic compounds, applied without mordant	Cotton, rayon, and other cellulosic fibers	Surfactant, defoamer, leveling and retarding agents, finish, diluents	70–95

Table 2. *Cont.*

Category of Dye	Features	Fiber	Pollutant	Dyes Fixation
Dispersive	Insoluble in water	Polyester, acetate, modacrylic, nylon, polyester, triacetate, and olefin fibers	Phosphates, defoamer, lubricants, dispersants, diluents	80–92
Val	Oldest dyes, chemically complex, water-insoluble	Cotton, wool, and other cellulosic fibers	Alkali, oxidizing agents, reducing agents, color	60–70

These pigments comprise of a double bond between two nitrogens (–N=N–), which is further linked to two aromatic group moieties such as naphthalene/benzene rings [84]. AzDs are positively charged at pH 6.8 and negatively charged at a higher pH, which affects their adsorption on semiconductor surfaces. The pH of the effluent is not neutral, and the mixture of substances that would have dissolved in water varies the surface characteristics of the semiconductor. When charged species are present in solution, an electrical double layer forms, affecting electron–hole pair separation and dye adsorption properties on the semiconductor surface. pH and the amount of dye present influence the rate of photocatalytic dye abasement [85]. They have amphoteric properties. Depending on the pH of the medium, AzDs can be anionic (deprotonation in the acidic group), cationic (extension in the amino group), or non-ionic [86]. The most known AzDs are acid dyes, basic dyes (cationic dyes), direct dyes (substantive dyes), disperse dyes (non-ionic dyes), reactive dyes, vat dyes, and sulfur dyes. Acidic dyes acquire their name from the fact that they are frequently employed to dye nitrogenous textiles or fabrics in inorganic or organic acid solutions. Cations that are extensively utilized in the manufacturing of acrylic and modacrylic fibers are produced by basic dyes in the solution. Electrostatic forces are used to apply direct dyes to fibers/fabrics in an aqueous medium containing ionic salts and electrolytes [87]. Anaerobic conditions can also contribute to the deterioration of the azo bond, which leads to the removal of pigments, but also leads to an insufficient mineral formation of harmful and carcinogenic products [88].

3.2. Dye-Degradation Mechanisms

The degradation mechanism had been discussed in detail in the literature in various citations; only one is mentioned here [89]. When aqueous titania is subjected to the visible-light irradiation greater than 3.2 eV (band gap), the electrons of the conduction band (electrons $_{CB}{}^{-}$) and the holes of the valence band (holes $_{VB}{}^{+}$) are created. These light-generated electrons (e^{-}) can either react with e^{-} acceptor O_2 adsorbed on the surface of TiO_2, or they can reduce the dye; they can also dissolve in water, causing reduction and producing an anion which could be a superoxide radical—$O_2^{\bullet -}$. The holes that are generated have the tendency to oxidize any organic molecule to R^{+}, and they can also oxidize water or hydroxyl ion to $OH^{\bullet}$ radicals. All these radicals along with titania have the potential to decompose dyes photocatalytically. The series of reaction schemes is given below [90] by Scheme 1. The pictorial representation of the dye-degradation mechanism is represented in Figure 2.

$$\text{Photocatalyst} + h\nu \rightarrow (e^{-}CB + h^{+}VB) \quad (1)$$
$$e^{-}CB + O_2 \rightarrow O_2^{\bullet -} \quad (2)$$
$$H_2O + O_2^{\bullet -} \rightarrow OOH^{\bullet} + OH^{-} \quad (3)$$
$$2OOH^{\bullet} \rightarrow O_2 + H_2O_2 \quad (4)$$
$$O_2^{\bullet -} + \text{dye} \rightarrow \text{dye}^{-}OO^{\bullet} \quad (5)$$
$$OOH^{\bullet} + H_2O + e^{-}CB \rightarrow H_2O_2 + OH^{-} \quad (6)$$
$$H_2O_2 + e^{-}CB \rightarrow OH^{\bullet} + OH^{-} \quad (7)$$
$$H_2O_2 + O_2^{\bullet -} \rightarrow OH^{\bullet} + OH^{-} + O_2 \quad (8)$$

$$\text{Dye} + h\nu \rightarrow \text{dye}^{*} \quad (9)$$
$$OH^{\bullet} / O_2^{\bullet -} / \text{dye}^{*} + \text{photocatalyst} \rightarrow \text{Dye degradation} + \text{products} \quad (10)$$

Scheme 1. Reaction scheme for the degradation of dyes using TiO_2 [90].

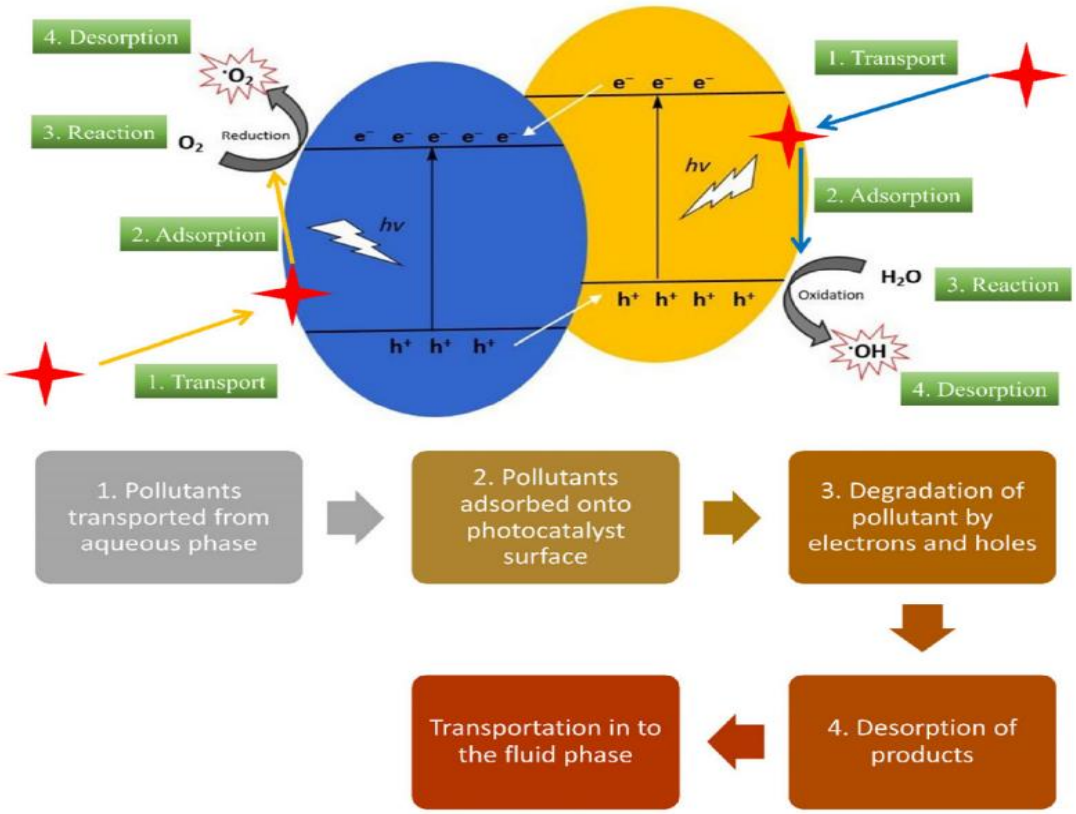

Figure 2. The process of dye-degradation mechanisms by photocatalysis, depicted graphically [91].

On the other hand, indirect methods can be used for the degradation mechanism, such as electron spin, resonance test scavenging, and radical trapping [92,93].

3.3. Technologies or Methods for the Removal of Dyes

There are innumerable dye-elimination techniques, which can be categorized as physical, chemical, and biological. The physical methods comprise of adsorption, ion exchange, and filtration/coagulation [94–100], whereas the biological include anaerobic deterioration, bio-sorption, and many more, while the chemical consist of ozonation, Fenton reagent, and photocatalytic processes, respectively [101,102]. The methodologies adopted for the removal of dyes is described in Figure 3.

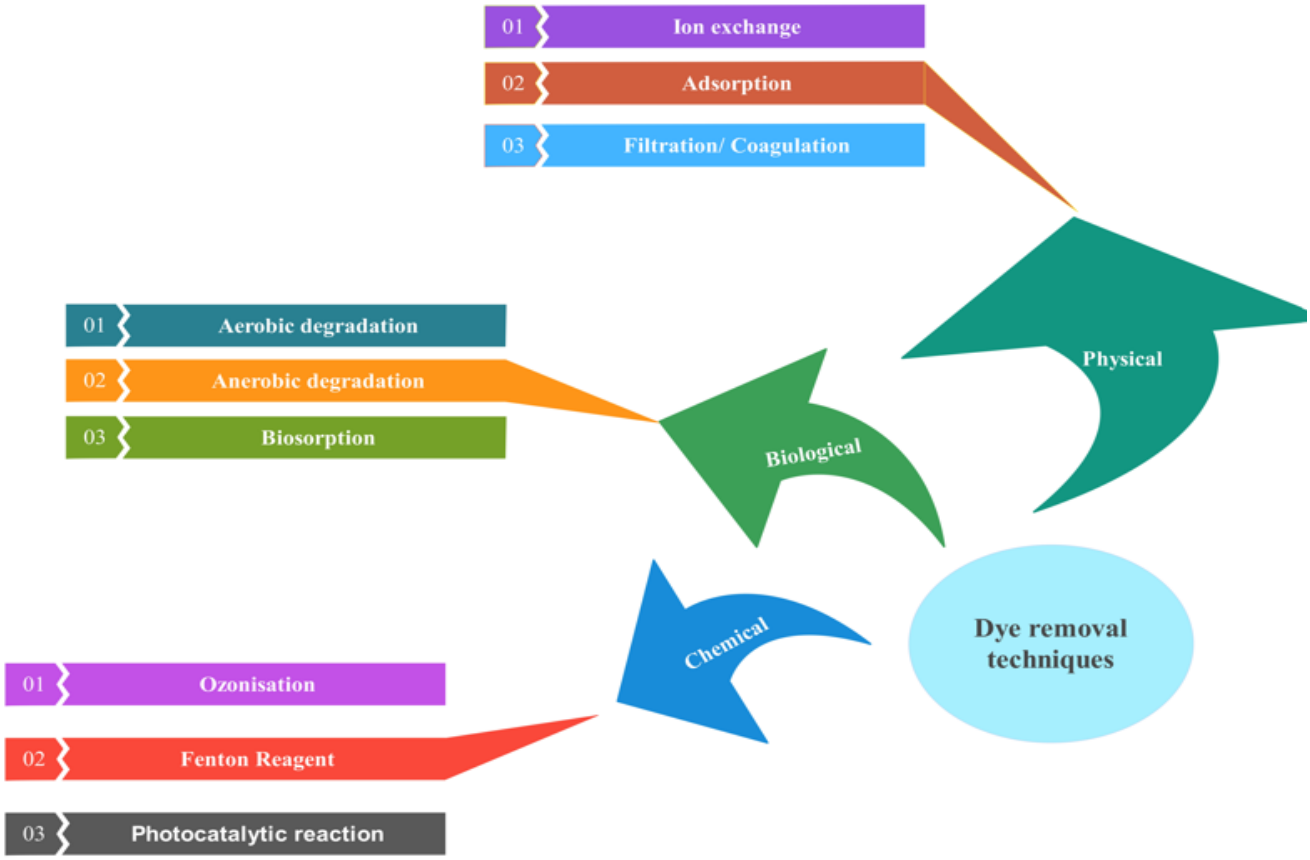

Figure 3. Different methodologies adopted for the removal of dyes.

In the physical method, different processes are used in the treatment of dyes, such as testing, mixing, precipitation, adsorption, and membrane filtration [97,103–105] (Table 3). Studies have shown that adsorption is the best method for the removal of dyes as it is simple, easily operative, highly efficient, cheap, and has been effective for toxic substances, whereas for membrane filtration, the contamination of the membranes and the cost of changing them are the biggest filtering limitations [106]. On the other hand, chemical treatments include coagulation-flocculation, oxidation, ozonation, Fenton oxidation, photocatalytic oxidation, irradiation, ion exchange, and electrochemical treatment [107,108]. These chemical methods are very effective in enabling the possibility of dyes removal, but excessive use of the chemicals causes difficulty in disposing of them into mud. Their disposal is too costly, and a reasonable amount of electrical power is required for these processes [109]. Biological analysis includes aerobic, anaerobic, and anaerobic–aerobic investigation, in which natural contamination is reversed into harmless and solid objects. The physicochemical and biological treatment of polluted water are the standard for dye-removal methods [110].

Table 3. Illustration of various methods for removal of organic dyes.

Strategies	Methods	Advantages	Disadvantages	Ref.
Chemical	Electro-Fenton reagent Ozonation Photocatalysis	Effective decolorization of soluble or insoluble dyes No sludge production initiates and accelerates Azo bond cleavages	No diminution of COD values by extra costs Sludge formation Formation of byproducts release of aromatic amines High costs	[108,111]

Table 3. *Cont.*

Strategies	Methods	Advantages	Disadvantages	Ref.
Physical	Ion exchange Adsorption Filtration/coagulation	Good removal of wide variety of dyes Regeneration No absorbent loss Good elimination of insoluble dyes Low-pressure process	Non-selective to absorbate Non-effective for all dyes High costs of sludge treatment Quality not high enough for re-using the flood	[103–105]
Biological	Enzymes Microbes Aerobic and anaerobic degradation Biosorption	Reduces the amount of waste that is delivered to landfills or incinerators Manufacturing requires less energy When it breaks down, it releases less hazardous compounds	Low biodegradability of dye Salt concentration stays constant	[98]

3.4. Stability of Non-Metal-Doped Titania

Non-metal-doped TiO_2 possesses higher catalytic activity in comparison to the undoped titania, as they have the enhanced capability of absorbing visible light, hence, more enhanced photocatalytic activity. Furthermore, the band gap becomes narrow because the lattice of titania is being substituted by oxygen. Almost all the non-metals reduce the re-connectivity of the e^-/h^+ duos but also decrease the band gap energy of titania via the formation of aperture energy. Therefore, the doping of non-metals in TiO_2 is an approach to increase the catalytic activity and the visible-light harvesting capacity. Therefore, it is safe to say that non-metal-doped titania can turn out to be the active catalyst for a visible-light catalyst for the degradation of different dyestuff [112]. Practical applications of nitrogen-doped TiO_2 for dye-sensitized solar cells were reported by Wei Guo and his co-workers, as N-doped titania dye-sensitized solar cells have shown 10.1% more conversion efficacy and are more stable because of the induction of N into the titania photo-electrode [113]. Carbon (C) and boron (B) co-doped photosensitizers have also been reported in the literature for efficient applications [114].

4. C-Doped TiO_2 (C/TiO_2)

The exploration of carbonaceous-doped materials with TiO_2 plays a significant role in photocatalysis, and they have shown spectacular growth due to their very simple method of synthesis [115]. Three dimensional cariogenic dot/TiO_2 nanoheterojunctions photocatalyst was synthesized by the hydrolysis process for the degradation of RhB, with different weight percent of C-dots for enhanced photocatalytic activity w [116]

The C/TiO_2 was immobilized with polyamide fibers with different weight percentages (1 wt.%, 2 wt.%, and 3 wt.%); the surface area of TiO_2 increased and the band gap energy (2.38 eV) decreased measurably after doping with non-metal for the degradation of MB [57]. The addition of C atoms to the TiO_2 structure can improve visible-light absorption by narrowing the band gap. However, organic chemicals, different dyes, and medicines were removed using C/TiO_2 photocatalyst matrices derived from aqueous [117]. The C/TiO_2 with several forms of carbon precursors was reported [118]. The most utilized carbon precursors are difficult to detect since the researchers use a variety of chemicals for titanium precursors, such as titanium carbide, titanium (IV) oxacetylacetonate, and titanium (IV) butoxide (TBOT) to act as TiO_2. The recombination of e^-/h^+ pairs is reduced by doping titania with carbon. Titanium dioxide (TiO_2) nanoparticles (NPs) were synthesized by sol-gel synthesis and doped with polydiallyldimethyl ammonium chloride (PDADMAC), as the carbon precursor caused a significant decrease in the band gap from 2.96 eV to 2.37 eV [41].

Recently, C/TiO_2 with anatase/rutile multi-phases coated on granular activated carbon was used under visible light for the removal of nonylphenol. A significant doping effect was observed in the band gap, which saw a decrease from 3.17 eV to 2.72 eV, respectively [119,120]. Indeed, carbon-based (nano) composites have improved photocatalytic activity due to the coupling effect from the incorporation of carbon species. However, several types of carbon–TiO_2 composites such as C-doped TiO_2, N–C-doped TiO_2, metal–C-doped TiO_2, and other co-doped C/TiO_2 composites have been reported (Table 4), which were synthesized by the solvothermal/HT method and sol-gel process [121].

Table 4. Methods and precursors used for the synthesis of C-doped TiO_2 photocatalysts.

Methods	TiO_2 Precursor	Carbon Source	References
Chemical bath deposition (CBD)	Titanium isopropoxide (TTIP)	Melamine borate	[122]
Sol-gel	Titanium isopropoxide (TTIP)	Microcrystalline cellulose (MCC)	[58]
Hydrothermal	TiC	-	[123]
Sol-gel	TTIP, TBOT, $TiCl_4$, $TiCl_3$	Ethanolamine (ETA), glycine, polyacrylonitrile (PAN), polystyrene (PS), starch, TBOT	[124,125]
Solvothermal treatment and calcinations	$TiCl_4$	Alcohols (benzyl alcohol and anhydrous ethanol)	[126]
Solvothermal	TTIP	Acetone	[127]
Electrospinning followed by heat treatment	TTIP	Acetic acid	[128]
Hydrolysis	TBOT	Glucose	[129]
Sol-gel	Titanium butoxide	-	[30]
Hydrothermal route	-	Various carbon sources	[42]

The C/TiO_2 photocatalyst exhibits enhanced photocatalytic activity in comparison to titania because the catalyst alters the crystal structure, lowers the pH, and narrows the band gap. C/TiO_2 supported by granular activated carbon for photocatalytic degradation of nonylphenol and anatase ratio is much better for the degradation in comparison to rutile [130]. Furthermore, it was discovered that annealing can increase the crystallinity of C/TiO_2 nanotubes, as shown in Figure 4 in the presence of Argon (Ar), instead of oxygen or nitrogen [131]. In addition, Ar or N_2 has proven beneficial in increasing the photocatalytic activity. The recombination of e^-/h^+ pairs is reduced by doping titania with carbon. TiO_2 nanoflakes (TNFs) and C/TiO_2 nanoflakes (CTNFs) were synthesized by the HT method, which is superior (92.7%) in the degradation of MB [40].

C/TiO_2 composites were further modified with nitrogen (as N–C-doped TiO_2 composites), and it was observed that N–C-doped TiO_2 composites exhibit improved photocatalytic activity as compared to only C/TiO_2 nano-formulations. High meso-porosity and a well-defined large surface area (102 m^2 g^{-1}) were obtained by N–C-doped TiO_2 composites synthesized by the solvothermal method with high photocatalytic evaluation [132–135]. In visible light, the catalytic image functions of non-metal-doping photocatalysts with different colors as model compounds are commonly used to analyze irradiation; however, this strategy has already been reported in the literature as an ineffective method [136]. This is due to the dye's ability to absorb visible light, which means that the photocatalytic process may not be driven solely by visible-light absorption. However, this is not only by the photocatalyst, but also by the dye's absorption of light (that is, dye sensitization). The most employed dyes in the literature are on visible-light active photocatalysts. In addition, Song and his colleagues reported a C-doped TiO_2/carbon nanofiber film (CTCNF) under visible-light irradiation for the breakdown of rhodamine B (RhB). The dye started to degrade, and its discoloration rate was 66.4–94.2% after 150 min of visible-light irradiation [137].

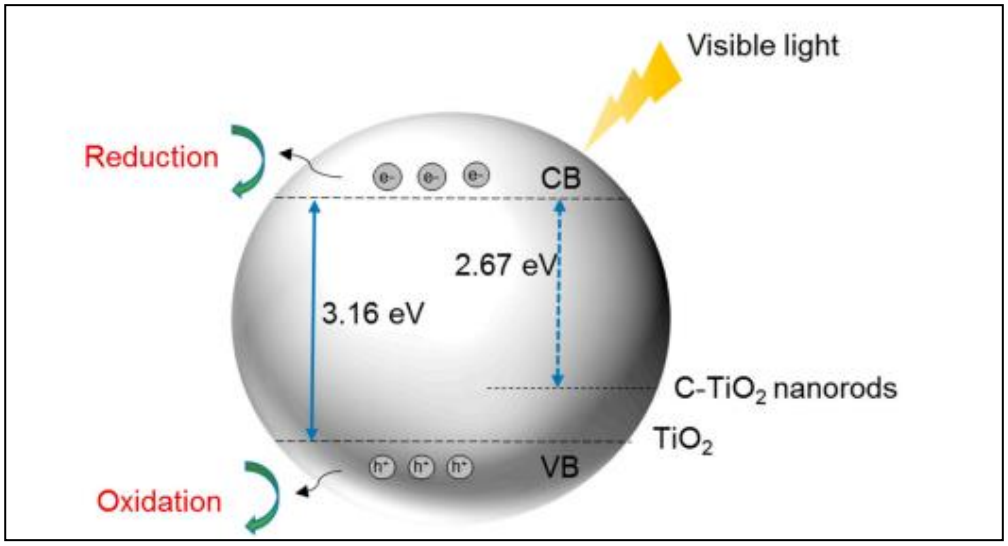

Figure 4. Photocatalysis mechanism of C-doped TiO_2 nanorods under visible light, adopted from [56].

In addition, the removal of other organic substances from pharmaceuticals, personal care items, and even microbes from water and hydrogen production are the best examples of compounds being removed with the help of a C/TiO_2 photocatalyst. C-TiO_2/rGO is used to form a hybrid nanocomposite that exhibits excellent photocatalytic activity for the better production of H_2 instead of pure TiO_2, as shown in Figure 5 [127].

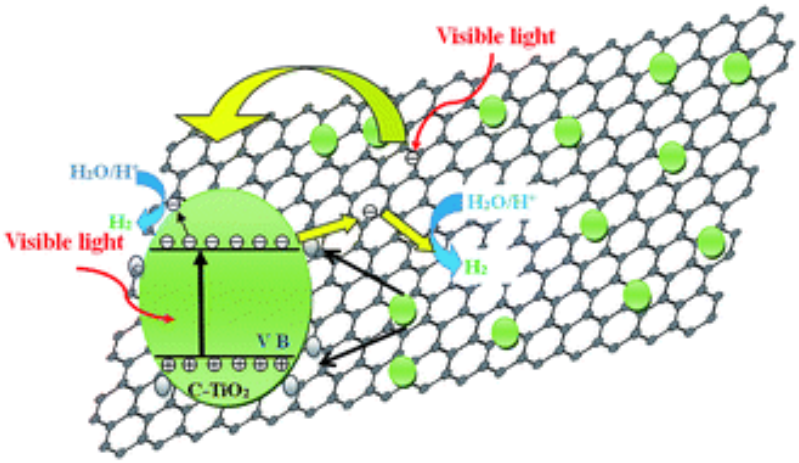

Figure 5. Photocatalytic mechanism of C-TiO_2/rGO adopted from [127].

The C/TiO_2 photocatalyst was prepared by the sol-gel process by using microcrystalline cellulose (MCC) as a carbon source material. In comparison to pure and C-TiO_2 a reduced band gap was observed. On the other hand, when Fe is co-doped with C-TiO_2 further reduction in the band gap exhibit stronger visible light absorption [138]. Some other carbon material, such as graphdiyne, plays a significant role in a variety of applications [139,140].

5. N-Doped TiO_2 (N/TiO_2)

Nitrogen is the most often-utilized non-metal dopant among all non-metal dopants [130]. N/TiO_2 has been reported (Table 5) for various photocatalytic applications [141–145]. Nitrogen (N) doping in TiO_2 nanotubes was prepared by the hydrothermal process for the degradation of dye and H_2 gas evolution. Urea was used as a N source, and optimized N/TiO_2 nanotubes (TiO_2 nanotubes vs. urea at 1:1 ratio) showed the highest degradation

efficiency over methyl orange (MO) dye (~91% in 90 min) and manifested the highest rate of H_2 evolution (~19,848 μmol $h^{-1} \cdot g^{-1}$) under solar-light irradiation [67].

N/TiO_2 was synthesized by the direct hydrolysis of titanium tetraisopropoxide and ammonia as a nitrogen source for the photocatalytic degradation of organic dyes in liquid phase with visible light. A batch photo-reactor was used to study the photocatalytic evaluation of methylene blue (MB) dye degradation under the optimum operating parameters to obtain the maximum efficiency toward dye degradation. The band gap energy of titanium dioxide was shifted toward a lower band gap, i.e., in the visible range from 3.3 to 2.5 eV. This is because of its low ionization energy and the atomic size being comparable to the size of oxygen [146]. As proven within Table 5, quite a few nitrogen precursors were used in the synthesis of N-doped TiO_2.

The photocatalytic activity of N/TiO_2 and N-doped TiO_2 with transition metals (Fe, Cu) was reported for the degradation of MB under sunlight [147]. N/TiO_2 showed the highest activity among the doped TiO_2 nanoparticles (0.006 min^{-1}). Titanium nitride/nitrogen-doped titanium oxide (TiN/N-doped TiO_2) composite films were synthesized by the sputtering process. A Raman spectral analysis revealed the formation of TiO_2 with anatase, which later transformed to the rutile phase, but the results showed that the photodegradation efficiency of MB was higher in the case of titania anatase after exposure to visible light [65].

Table 5. Summary of N-doped TiO_2 photocatalysts synthesized by variety of methods and source precursor materials.

Year of Study	Method	TiO_2 Precursor	Nitrogen Source	Ref.
2017	Addition of N source to the TiO_2 precursor solution	TBOT	Tetra methyl-ethylene-diamine	[148]
2020	CVD	$TICl_4$	Tert-butylamine, benzyl amine	[149]
2017	Hydrothermal	TBOT	KNO_3	[150]
2019	Hydrolysis	TTIP	NH_4Cl, pyridine	[151]
2016	Electrochemical	Titania nanotubes	Diethylenetriamine, ethylenediamine, hydrazine	[152]
2019	Sol-gel	TTIP, TBOT, $TiCl_4$, Titanic acid	Urea, NH_3, nitro methane, n-butyl amine, N_2, hydrazine, HNO_3,	[153]

For the solar-driven photocatalysis over Ti^{3+} and N co-doped photo catalysts, Cao et al. [154] proposed a modified mechanism. The materials were made by reducing urea-modified mesoporous TiO_2 spheres with $NaBH_4$ at 350 °C in an Ar environment. The above-mentioned N-doping of TiO_2 resulted in the emergence of a new impurity level above the VB. In addition, by introducing Ti^{3+} and O below the CB, an intermediate energy level was created. As a result, the band gap was decreased, which increased photocatalytic effectiveness in the visible light. The schematic diagram of N-doped TiO_2 is shown in Figure 6.

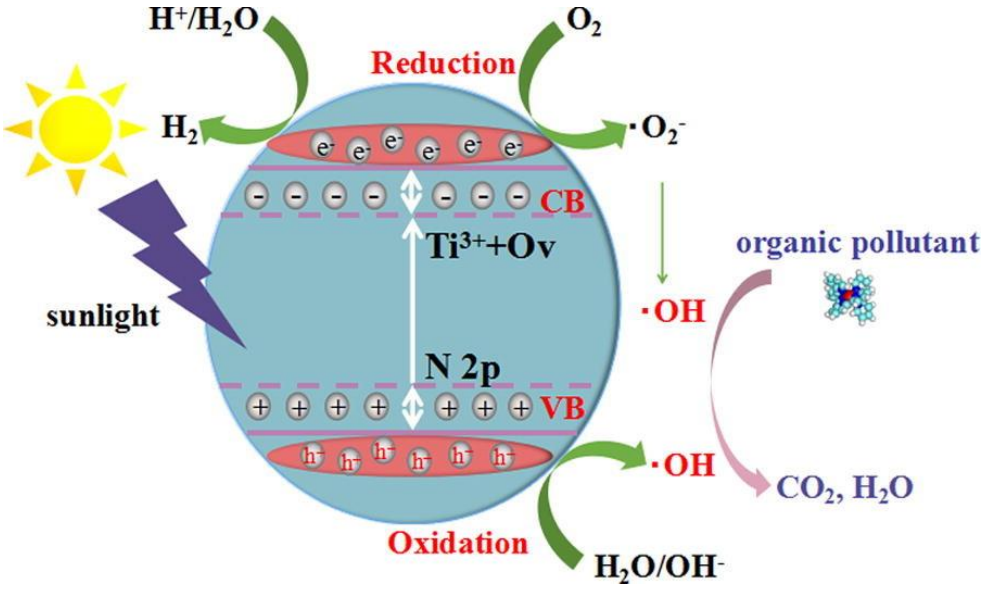

Figure 6. N-doped TiO_2 photocatalytic process driven under the sun is schematically represented [154].

The activity of N-doped TiO_2 as a photocatalyst has been examined in various studies. In general, N/TiO_2 photocatalysts have been utilized to remove organic chemicals from water, namely dyes and medicines, but phenol, furfural parabens, surfactants, and herbicides were among the other pollutants that were destroyed using doped TiO_2 with N [155]. It was also suggested that N/TiO_2 photocatalyst could be used to remove pollutants from the gaseous phase, such as acetaldehyde, benzene, ethylbenzene, NH_3, and NOx. Antibacterial characteristics were found in some of the photocatalysts, such as against Escherichia coli and oral cariogenic biofuels. Furthermore, the use of N-doped TiO_2 for human breast cancer diagnostics, and cancer treatment such as for melanoma, has been reported previously in Figure 7 [156]. N/F co-doped mp TiO_2 has been shown to have the highest adsorption and photocatalytic activity. The solvothermal method was adopted for the synthesis of N/F mp TiO_2 by using urea as a nitrogen source and ammonium fluoride as a fluorine source [29] The L-amino acid (C-N co-doped or C-N-S tri-doped) -TiO_2 photocatalyst was used for dyes removal under visible dye. The photodegradation of methyl orange and direct red 16 was studied by the first order kinetics, and the rate constant for DR16 photocatalytic removal using L-Arginine (1 wt.%)-TiO_2 was 2.9 and 4.3 times greater compared to those of L-Methionine (1.5 wt.%)-TiO_2 and L-Proline (2 wt.%)-TiO_2, respectively [157].

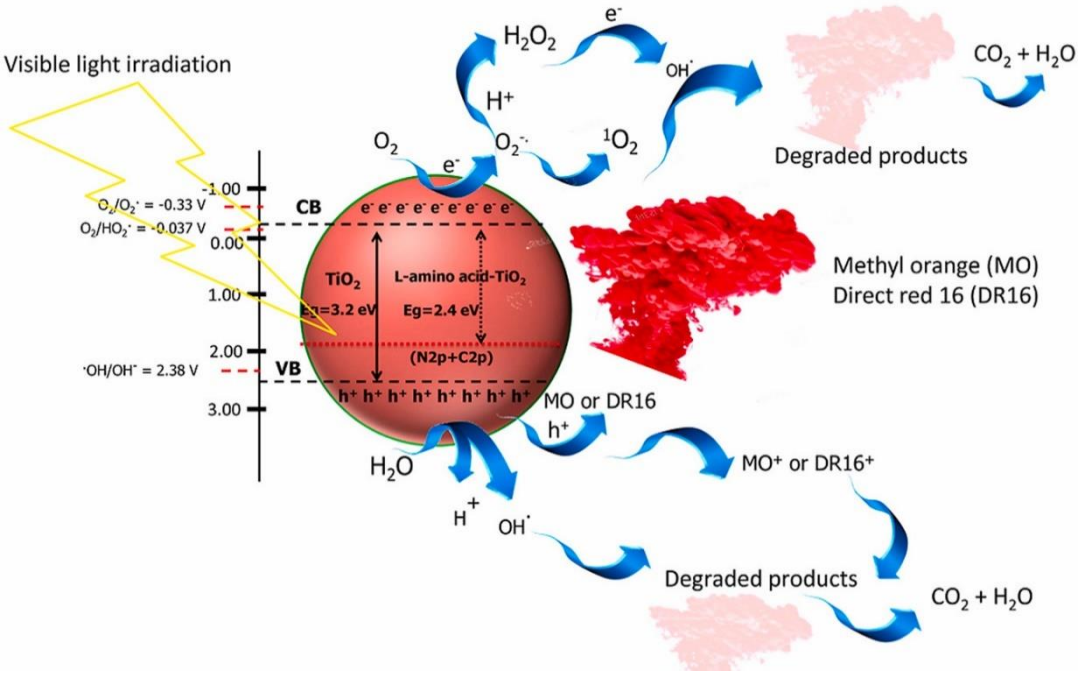

Figure 7. N-doped TiO_2 photocatalytic [157].

6. S-Doped TiO_2 (S/TiO_2 or SdT)

Amongst all the non-metals, sulfur would have been difficult to dope with titania because a large amount of formation energy is required for the replacement of S with O in titanium dioxide [158]. In contrast to the previous statement, S/TiO_2 (SdT) (anatase) was synthesized using TiS_2 (titanium disulfide) by the oxidative annealing. Therefore, this doping led to the red shift in the absorption band of SdT rather than the undoped titania. Furthermore, it was used for the photocatalytic degradation of methylene blue (MB). SdT instigated MB's irradiation quite efficiently in the visible-light region, as shown in Figure 8 [159]. SdT was also prepared by the heating of powder TiS_2 in the solution of HCl at 180 degrees, a comparatively lower temperature in comparison to the conventional methods of synthesizing SdT. Traditionally, it has been prepared by the thermal decomposition of thiourea (ThU) at elevated temperatures, whereas ThU is the source of sulfur. The formulated SdT at a demoted temperature was used for the desolation of 4-chlorophenol; it was concluded that the one-step hydrothermal process for the production of SdT was successful for the irradiation of 4-chlorophenol by visible-light photocatalytic activity [160].

Sulfur-doped and sulfate TiO_2 (SdST) were synthesized using the solvothermal method; potassium per sulfate (KPS) was taken as a source of sulfur and the irradiation rate of phenol was studied. As we know, titania showed lower photocatalytic activity in the visible light because it has a broad band gap energy, which limits the absorbance of UV light of less than 387 nm. However, the SdST catalyst showed higher degradation activity for phenol instead of pure TiO_2, especially in the range greater than 450 nm (longer visible-light range). Almost 51.3% of the containment (phenol) was degraded at a 0.5 ratio of the catalyst (SdST) for 10 h under the ranges, as mentioned in Figure 9 and Table 6 [161].

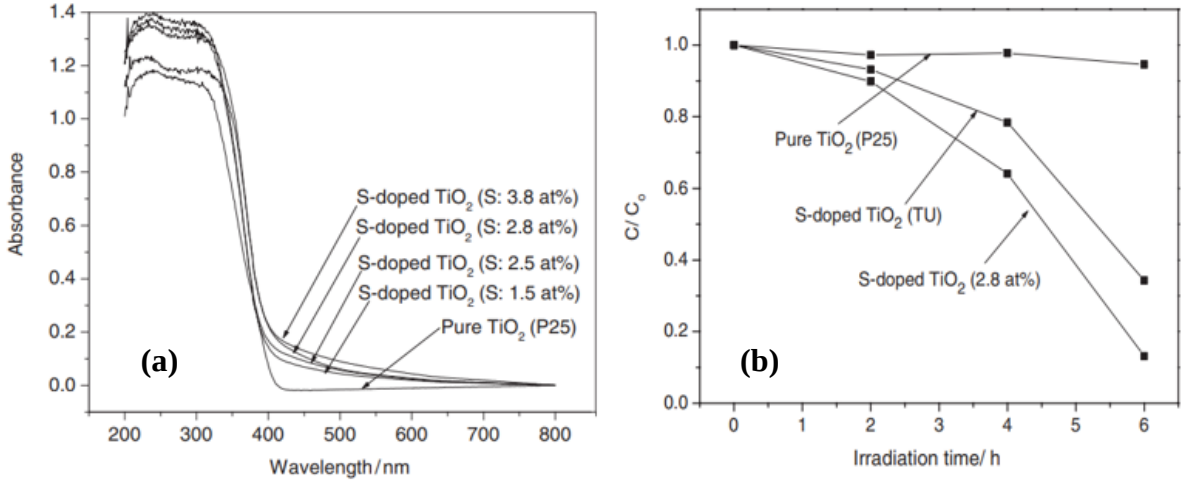

Figure 8. (**a**) Response of different concentrations of sulfur in S-doped TiO_2; (**b**) photocatalytic degradation of 4-chlorophenol by pure TiO_2, SdT prepared by ThU and SdT by hydrothermal process studied via UV-vis [160].

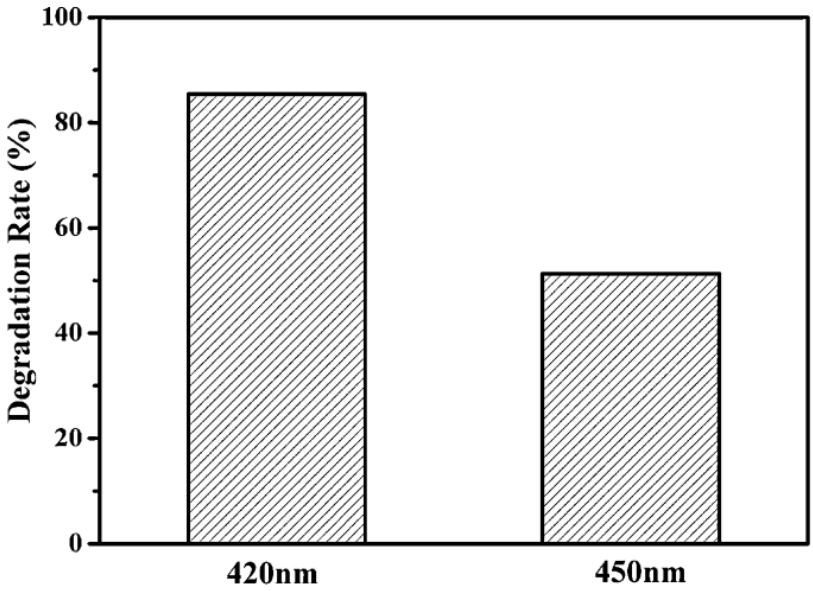

Figure 9. The photocatalytic degradation of phenol using SdST-0.5 at various wavelength irradiation [161].

Table 6. Summary of S-doped TiO_2 photocatalysts synthesized by variety of methods and source precursor materials.

Year of Study	Method	TiO_2 Precursor	Sulfur Source	Ref.
2003	Oxidative heating	Anatase	TiS_2	[159]
2006	Low-temp hydrothermal	Anatase	TiS_2 powder with HCl solution	[160]
2012	Solvothermal	TBOT	Potassium per sulfate	[161]
2016	Free oxidant peroxide method	Anatase	Thiourea (ThU)	[162]
2018	HT	Titanium sulfate ($TiOSO_4$)	$TiOSO_4$	[163]

7. P-Doped TiO_2 (P/TiO_2 or PdT)

In the recent years, P/TiO_2 (PdT) has gained attention because of their potential to increase the surface area, restrain the transformation of anatase to rutile, enhance the absorption of visible light and decrease grain growth [164] (Table 7). Therefore, many

studies have been conducted for the generation of PdT and to study their properties regarding water splitting [165], dye-degradation, etc. [166]. Similarly, the synthesis of PdT nanoparticles using the sol-gel process was performed. The results showed a remarkable increased activity of the degradation of MB because of high visible-light pursuit, and the ESR spectroscopy (electron spin resonance) deduced its refined charge separation [167].

The fabrication of P doped over titania nanofibers (PdTNFs) was first reported by Zhu. Y. et al., from the method known as chemical vapor deposition (CVD), which showed remarkable results for electrochemical water splitting [168]. The doping of phosphorous decreases the band gap of titania and creates disproportion between O_2 and Ti^{4+} charges; therefore, the recombination of charge carriers is hindered. In TiO_2 (anatase type), the substitution of P^{3-} over O^{2-} is much greater than substituting P^{5+} onto Ti^{4+} (1.32 eV) because it requires high formation energy (15.48 eV). Hence, it shows that the incorporation of P^{5+} into titania lattice is achievable by forming the Ti-O-P bond rather than the Ti-P bond [169]. The separation of charges in the photocatalytic phenomenon is facilitated by the phosphate ions, which act as an electron-withdrawing species [170].

The photocatalytic activity of sulfamethazine (SMHZ) was investigated using mixed oxide novel-doped Fe_2O_3 and TiO_2. The weight percentage of 1.2 of mixed oxide had successfully degraded 30% of SMHZ; the percentage degraded is much higher than Fe_2O_3-TiO_2 or pure TiO_2 (Figure 10). [171].

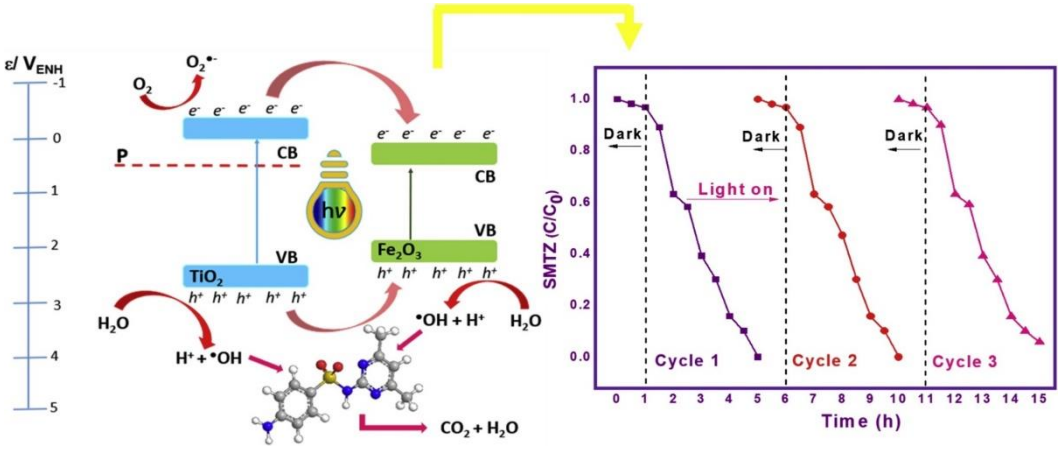

Figure 10. Photocatalytic mechanism of P-doped Fe_2O_3-TiO_2 against SMHZ [171].

Table 7. Summary of P/TiO_2 photocatalysts synthesized by variety of methods and source precursor materials.

Year of Study	Method	TiO_2 Precursor	Phosphorous Source	Ref.
2020	Chemical vapor deposition	Titanium (IV) butoxide ($Ti(OC_4H_9)_4$)	Red phosphorous	[171]
2014	Sol-gel method	TBO	Phosphorous acid	[172]
2011	Sol-gel process	Silicate/TiO_2 NPs	Phosphoric acid (H_3PO_4)	[164]
2009	Sol-gel	TBO	H_3PO_4	[173]

8. B-Doped TiO_2 (B/TiO_2 or BdT)

The non-metal doping of anatase TiO_2 was further doped with B, C, N, and F [174–176]. The B/TiO_2 hybrid hollow microspheres were synthesized by hydrothermal treatment. This boron-doped titania photocatalyst was used for MB degradation in aqueous solution and served as a target pollutant to evaluate the photocatalytic activity under sunlight. A higher photocatalytic activity of boron-doped hybrid hollow microspheres was observed (Table 8), which was comparatively much greater than undoped titania [177].

B/TiO_2-nanotubes (B/TiO_2NTs) were synthesized by the electrochemical anodization method with boron concentrations of 70, 140, 280, and 560 ppm and activated via UV-visible irradiation. The results showed that the dye-degradation rate of Acid Yellow1 (AY1) was twice greater at the doped electrode, which contained 280 ppm of B, and the activation of the electrode was maximum there, as observed from the UV-visible light. When the AY1 (100 ppm) was treated at the B/TiO_2NTs electrode for 120 min at +1.2 V, pH 2 and in 0.01 mol L^{-1} of sodium sulfate solution (Na_2SO_4), 100% discoloration of the dye was observed. Therefore, the synthesized amalgamation has the potential to become a stable electrochemical catalyst [178].

The synthesized BdT nanostructures was carried out using the sol-gel method. Studies have shown that, after the doping of boron, the band gap decreased from 2.98 eV of undoped titania to 2.95 eV of B/TiO_2 (7% boron content) (Figure 11a). Boron has the tendency to occupy the interstitial sites in the crystal lattice of TiO_2 and forms a Ti-O-B bond. Therefore, the degradation studies of 4-nitrophenol were studied using the said nanoformulations. The results showed that BdT (7%) displayed a 90% degradation efficacy compared to the undoped titania (79%) because the Ti-O-B linkage has a synergistic effect on supplementing the catalytic activity, as shown in Figure 11b [179].

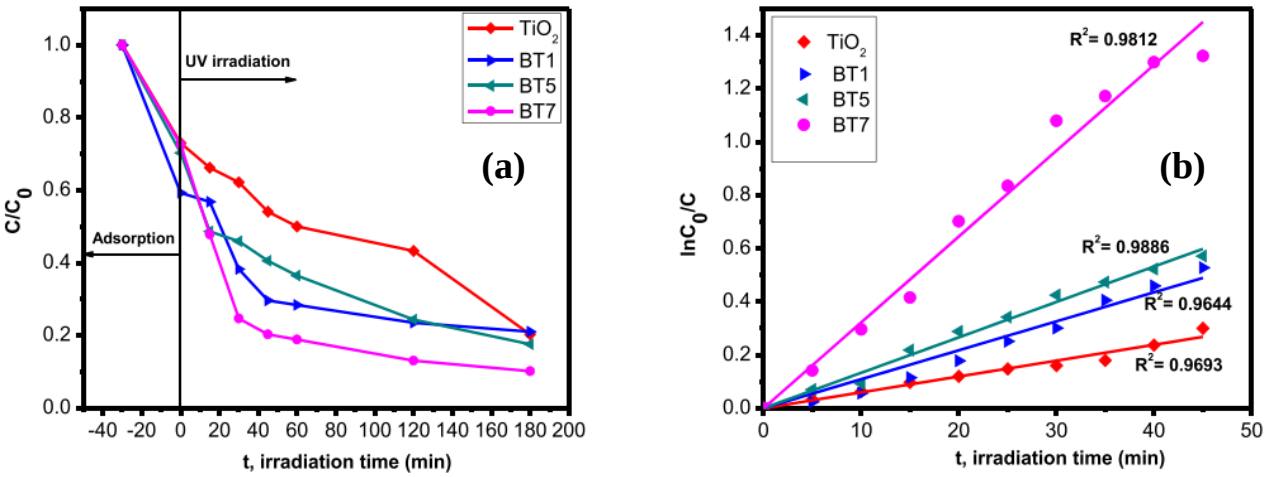

Figure 11. (**a**) Photocatalytic degradation of 4-nitrophenol using B/TiO_2 and undoped TiO_2. (**b**) First-order plot of photocatalytic degradation of 4-nitrophenol using UV-visible-light irradiation in the presence of BdT and undoped TiO_2 [171].

Table 8. Summary of B/TiO_2 photocatalysts synthesized by variety of methods and source precursor materials.

Year of Study	Method	TiO_2 Precursor	Boron Source	Ref.
2020	Sol-gel	Titanium isopropoxide	Boric acid	[179]
2015	Electrochemical anodization	Titanium sheets	$NaBF_4$	[178]
2011	HT	$(NH_4)_2TiF_6$	H_3BO_3	[177]

9. Halogens-Doped TiO_2 (X = F, Cl, Br, and I)

The hydrogenated F/TiO_2 (FdT) nanocrystals were synthesized using the physico-chemical method. F-doping has the potential to increase the surface area of TiO_2; further, hydrogenation plays a pivotal role in forming the F-H and O-H bonds on the surface of titania and creating vacancies of Ti^{3+} and O^{2-}, which increases the range of absorption alongside the light utilization capacity of TiO_2. The bonds O-H and F-H can favor trapping the holes and can also react with water to produce an active species ($OH^{\bullet}$). Now, these hole and electron pairs can easily be separated to participate in the photocatalysis. Irradiation

studies of MB were conducted and showed that the degradation rate constant of hydrogenated FdT is 0.146 min^{-1}, which is almost twice the rate of pure TiO_2 (0.063 min^{-1}) [180].

Hydrogen and fluoride co-doped TiO_2 nanostructures have been made from annealing. The doping of halogens decreases the band gap and bestows the oxide material a greater absorbance capacity. The results demonstrated that FdT is a better photocatalyst, as shown in Figure 12 and Table 9 [181].

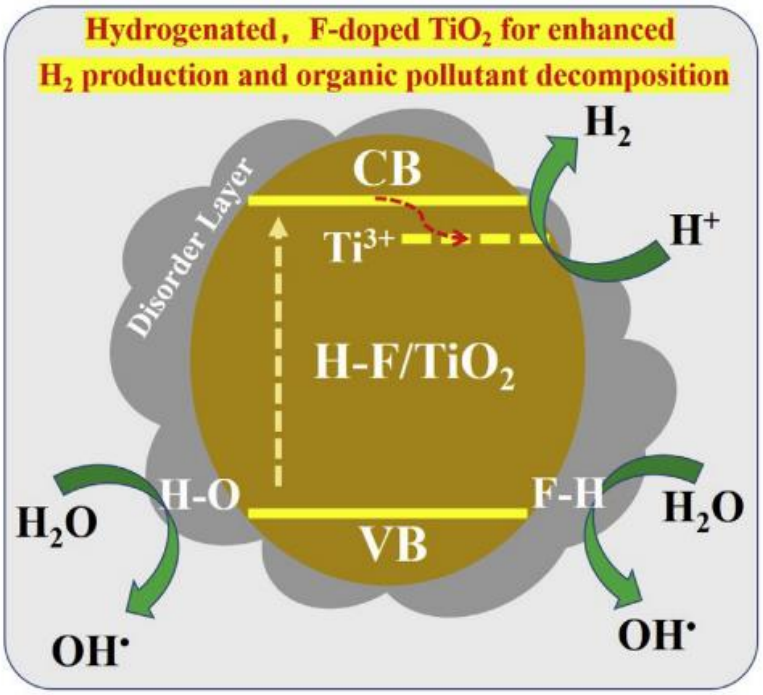

Figure 12. Suggested photocatalytic degradation for H_2 production and dye degradation [180].

Table 9. Summary of halogens-doped TiO_2 photocatalysts synthesized by variety of methods and source precursor materials.

Year of Study	Method	TiO_2 Precursor	Fluorine Source	Ref.
2020	Oxidative annealing	Titanium isopropoxide	NH_4F	[181]
2019	Physicochemical	TTIP	NH_4F	[180]
2017	Sol-gel	Titanium isopropoxide	Trifluroacetic acid	[182]
2014	Sol-gel	Tetrabutyl titanate	NH_4F	[183]
Year of Study	**Method**	**TiO_2 Precursor**	**Chloride Source**	**Ref.**
2020	Oxidative annealing	Titanium isopropoxide	NH_4Cl	[181]
2012	Sonochemical synthesis	Tetraisopropyl titanate	NaCl	[184]
2008	Hydrolysis	Tetrabutyl titanate	HCl	[185]
Year of Study	**Method**	**TiO_2 Precursor**	**Bromide Source**	**Ref.**
2017	HT	TBOT	NH_4Br	[186]
2009	Sol-gel	TBOT	Cetyl trimethyl Ammonium bromide (CTAB)	[187]
2004	HT	Titanium chloride	Hydrobromic acid	[188]
Year of Study	**Method**	**TiO_2 Precursor**	**Iodide Source**	**Ref.**
2017	Sol-gel	Titanium (IV) ter-butoxide	Potassium iodide	[189,190]

A Cl/TiO_2 (CldT) photocatalyst was prepared, which shows greater absorption in the range of visible light. The doping of chlorine decreases the band gap of titania; therefore, the absorption spectra are extended. CldT shows better degradation of phenol than the pure one that is 42.5% after 120 min [185].

The synthesized Br/TiO_2 (BrdT) hollow spheres are made by the hydrothermal method. Studies have revealed that the adsorption peak of BrdT hollow spheres is near 517 nm, which is greater than that of undoped titania. The band enhanced towards the visible-light range. The band gap of the fabricated spheres decreased (1.75 eV), whereas the band gap of undoped TiO_2 was around 2.85 eV; this illustrates that the doping of Br instigates the impurity level between the conduction and valence bands; therefore, the transition of electrons is promoted [186].

I/TiO_2 photocatalysts were prepared via the sol-gel method. They tend to have higher photo-degradation potential under direct-sunlight irradiation. Without catalysts, the photocatalytic degradation of RhB was not observed. The mechanism of the photocatalytic degradation of RhB using I/TiO_2 involves the following steps as shown in Scheme 2 [189]:

$$I/TiO_2 + h\nu \rightarrow I/TiO_2(e^- + h^+)$$

$$I/TiO_2(h^+) + H_2O \rightarrow I/TiO_2 + H^+ + {}^{\cdot}OH$$

$$I/TiO_2(h^+) + OH^- \rightarrow I/TiO_2 + {}^{\cdot}OH$$

$$I/TiO_2(e^-) + O_2 \rightarrow I/TiO_2 + O_2^{-\cdot}$$

$$RhB + OH^{\cdot} \rightarrow products$$

Scheme 2. Reaction scheme for the degradation of RhB dye using I/TiO_2.

10. Si-Doped TiO_2 ($SidTiO_2$)

Scheme 2 is based on nanotubes for MO. The results showed that 5% $SidTiO_2$ has a higher catalytic efficacy for MO degradation than the tubes synthesized with titania [75]. Similarly, in another study, $SidTiO_2$ was synthesized using the hydrothermal method for the photocatalytic degradation of organic pollutant, phenol. The results showed a nine-times higher percentage degradation with $SidTiO_2$ than undoped titania nanotubes [191] (Table 10).

Table 10. Summary of Si/TiO_2 photocatalysts synthesized by variety of methods and source precursor materials.

Year of Study	Method	TiO_2 Precursor	Silicon Source	Ref.
2019	Hydrothermal	Commercial TiO_2	SiO_2 commercial	[191]
2017	Solvothermal	Titanium oxysulfate	Tetraethoxysilane	[75]

11. Factors Affecting the Degradation of Photocatalytic Activity

The photocatalytic degradation of dyes is strongly affected by consideration of the following parameters: pH, dye concentration, the size and structure of the photocatalyst, pollutants concentration and types, light intensity and irradiation time, dopants' effect on dye concentration, etc. These factors and their impact on the dye-degradation performance are demonstrated with details in this section.

11.1. Effect of pH

pH is a pivotal parameter that impacts the photocatalytic activity. Some of the results on the effect of pH on dye degradation are presented in Table 11 pH fluctuations in combination with calcinated non-metal-doped titania possess the best catalytic degradation

results because of the synergistic effect of phase structure and crystallinity [192]. The results reported in Table 11 show that the facet TiO_2 can be deprotonated/protonated under alkaline/acidic conditions, respectively. Therefore, it can be concluded that pH alterations can result in the escalation efficacy of the dye degradation of titania without influencing the rate equation [193]. The effect of pH on the decomposition of MO was investigated by Guttai N et al., and it turned out to be the first-order reaction rate, which was 25 times higher at pH 2 than at pH 9 [194]. This also means that some types of dyestuff are preferentially photo-degraded on TiO_2 surfaces. Dyes can be degraded in three ways as a function of pH: directing hydroxyl radical, (ii) the direct involvement of a hole in the oxidation reaction, and (iii) a tête-à-têtes reduction in the participation of the activated electron in the steering band [195]. The effect of pH on the photo-degradation efficiency of the dyes must be considered in conjunction with several other parameters. The interaction of hydroxide ions can produce hydroxyl radicals. At a low pH, holes are the dominant forms of oxidation, and at a neutral or high pH, hydroxyl radicals are the dominant species, respectively.

Table 11. Different types of dyes under optimum pH.

Dye Type	Light Source	Photocatalyst	pH Range	Optimum pH	Ref.
Orange G (OG)	UV	$Sn/TiO_2/Ac$	1.0–12.0	2.0	[196]
(OG)	Visible	$N\text{-}TiO_2$	1.5–6.5	2.0	[197]
Bromo-cresol purple (BCP)	UV	TiO_2	4.5 & 8.0	4.5	[198,199]
Methyl Red (MR)	Visible	$3\%Ag+1.5\%Ni\text{-}TiO_2$	3–10	4	[199]
Malachite Green (MC)	Sun light	$Ni/MgFe_2O_4$	2.0–10.0	4	[200]
Indigo Carmine (IC)	UV	TiO_2	4.0–11.0	4	[201]
Textile dye (TD)	UV	TiO_2	3.0–7.0	5	[202]
Basic Yellow 28 (BY28)	UV	TiO_2	3.0–9.0	5	[203]
Methylene Blue (MB)	UV	TiO_2ZnO	1.0–6.0	2	[204]
Reactive Blue 4 (RB4)	UV	Anatase TiO_2	3.0–13.0	3–7	[205]
Procion Yellow (PY)	UV	TiO_2	2.0–10.0	7.8	[206]
Acid Orange (AO)	UV	$WO_3\text{-}TiO_2$	1.0–9.0	3	[84]
Methyl Orange (MO)	UV	TiO_2	2.0–10.0	8	[207]
Rhodamine B (RhB)	UV	ZnO	2.0–12.0	12	[208]
MO, RhB	UV	ZnO	2.0–10.0	Basic medium	[209]

Hydroxide (OH^-) is easy to produce in an alkaline solution with an oxidizing ion, which then penetrates through the semiconductor surface. Therefore, the efficiency of the process increases reasonably [210]. According to the findings, pH plays an important role in altering the charges on the dyes; for example, BCP dye degradation was better in acidic media than in alkaline media [198]. Azo dyes are positively charged at pH 6.8 and negatively charged at a higher pH, which affects their adsorption on semiconductor surfaces. When charged species are present in a solution an electrical double layer forms, which affects the electron–hole pair separation and adheres the adsorption properties of the dye on the surface of the semiconductor. pH and the amount of dye present influence the rate of photocatalytic activity [85].

11.2. Effect of Dye Concentration

The optimum concentration of the dye is very important for the photocatalytic reaction, as it is highly dependent on the type of dye being considered. Generally, by increasing the concentration of the colorant, the photocatalytic degradation efficiency of the dyestuff will

decrease by suppressing the active sites, therefore, hindering the activity [211]. However, a small quantity of the dye is subjected to degradation and it only contributes to the process of photocatalysis. The initial concentration of the dye in the photocatalytic process is important to consider [81]. This is because as the dye concentration increases, more organic molecules are adsorbed on the surface of TiO_2, but fewer photons reach the catalyst surface, resulting in less OH production, and thus, lowering the percentage degradation [212]. On the other hand, the ionic behavior of dye molecules may result in either accelerating or slowing down the process of the degradation of dyestuff. Normally, metal ions are adsorbed on the surface of the photocatalyst and make them slightly positively charged. As this effect reduces the electrostatic repulsion for anionic dyes, they can be adsorbed and degraded readily in the presence of metal ions. On the contrary, a retarding effect can also be observed for cationic dyes due to the decrease in attraction between positively charged dyestuff and neutral or slightly positive catalyst surfaces [213].

11.3. Photocatalyst's Size and Structure

Surface morphology, such as particle size and agglomerate size, is an important component to address while discussing photocatalytic degradation, since there is a direct relationship between organic molecules and photocatalyst surface coverage. The speed of the reaction is determined by the number of photons striking the photocatalyst; therefore, it can be suggested that the reaction happens solely in the phase absorbed by photocatalysts [214]. Titania and Cu-TiO_2 nanocomposites were used to degrade MR. Studies have suggested that the Cu-modified titania shows more promising results for the catalytic degradation of MR in comparison to the titania because the morphology of the latter is different than the modified version of titania, which facilitates the advancement of organic molecules towards the catalyst [215].

11.4. Pollutant Concentrations and Types

The rate of the photocatalytic destruction of a pollutant is determined by the type of pollutant employed, along with its concentration and other chemicals present in the aqueous matrix. Many researchers have found that the rate of reaction of TiO_2 is influenced by the concentration contaminants present in water. High levels of water contaminants fill the TiO_2 site, reducing photonic efficiency, and moving the image of the catalyst towards malfunctioning [216]. The chemical structure of the target component, in addition to the concentrations of the pollutant, alters the photocatalytic degradation performance of the catalyst being used because of its conversion into its respective intermediates. For example, studies have shown that 4-chlorophenol takes longer to release irradiation than oxalic acid because it converts directly into carbon dioxide and water [217].

11.5. Surface Area of the Photocatalyst

The surface of TiO_2 is crucial in its employment as a photocatalyst because its reactions occur at the surface. This usually increases its availability either by utilizing it in the form of very fine particles, molding it into a porous sheet, or suspending it in some liquids [218]. Nanomaterials with a crystallite size/grain of less than 20 nm have gained particular interest among researchers because their physical characteristics differ significantly from their bulk counterparts. This has also opened new opportunities for their use as photographic catalysts in various fields. As the surface area of the image catalyst grows, more active sites become prominent [219].

11.6. Effect of the Intensity of Light and Irradiation Time

The intensity of light plays an important role in photocatalytic dye degradation, which results in the formation of less toxic byproducts of the dye under consideration. A large amount of research has been conducted on these specific parameters [220]. The effect of the intensity of light on the degradation and decolorization of RY14 is studied in [221]. The dye degradation is affected by both the strength of the light and the time it takes to expose it to

degrade the dye or pollutants [193]. As the intensity of light significantly increases, the dye degradation rate enhances; this is because of an increase in the number of photons striking per unit time per unit area of the photocatalyst. Conversely, by further increasing the intensity of light, there might be a chance of higher thermal effects [173]. It was confirmed that N/TiO_2 showed higher dye degradation (almost 60% in 6 h) under visible light. On the contrary, under sunlight irradiation, N/TiO_2 unveiled degradation efficiency that was a little higher as compared to the non-doped TiO_2 efficiency of degradation. A negative light intensity effect on Congo Red was studied when the light intensity varied from 50 to 90 $J{\cdot}cm^{-}$ [222].

11.7. Dopants' Impact on Dye Degradation

The main goal of doping is to cause a chromic change in the optical properties, which is defined as the reduction in the band gap or the introduction of intra-band gap conditions that leads to an increase in the absorption of visible light. Non-metal dopants' effects on photocatalytic activity is a challenging problem to tackle. The performance of TiO_2 can be improved by doping with non-metals to enhance the photocatalytic efficiency of titania. Depending on the type of dopants and its concentration, it can also allow light to be absorbed into the visible area at different levels. As a result, visible light can be used to stimulate photocatalysis on modified TiO_2. In mixed systems, dye deterioration is often much faster than systems alone, as the oxidation of dyes utilizes exciting holes quickly and effectively, reducing electron–hole regeneration [214]. The prime concentration of dyes for a photocatalytic reaction is a key parameter that is highly dependent on the type of dye employed. Typically, by increasing the pollutants concentration, the photocatalytic degradation efficiency deceases. The reason for this is that maximum or higher dye molecules compete for limited active sites along with turbidity increases [223].

11.8. Effect of Mass Loading on the Catalytic Activity

TiO_2 has been made to absorb lower-energy photons using a variety of approaches. Kaur et al., reported that under optimized conditions with the highest efficiency, the catalyst dosage for the maximum photocatalytic degradation of RR 198 is 0.3 g [224]. It is manifested that the photodegradation rate increases with the increase in the amount of photocatalyst and then decreases with the increase in the catalyst concentration [225]. In another study, an increase was reported in the weight of the catalyst from 1.0 to 4.0 g L^{-1}, which increases the dye decolorization sharply from 69.27% to 95.23% at 60 min and the dye degradation from 74.54% to 97.29% at 150 min. The optimum concentration of the catalyst for efficient solar photo decolorization and degradation is found to be 4 g/L [226].

12. Conclusions

This review focused on the comprehensive study of the fundamental aspects of non-metal-doped/TiO_2 nanoparticles. Titania is considered as the best visible-light-driven photocatalyst for the degradation of numerous dyes. Plentiful research has been carried out that encompasses the importance of non-metals-doped titania in comparison to the undoped TiO_2 for their better photocatalytic dye degradation of various anionic and cationic dyes, in order to overcome the environmental pollution issues via industrial effluents or other pollutants. We must incorporate most of the literature present on non-metals such as C, Si, N, P, B, halogens, etc. The effect of different parameters, for instance, pH, dyes concentration, photocatalyst's size and structure, pollutants concentration and types, the surface area of photocatalysts, the effect of light intensity along with its irradiation time, catalyst loading, variation in temperature, and doping (non-metals) impact with optimization has a strong correlation with pollutants degradation rate, which is also discussed in this review. The photocatalytic performance of non-metal-doped titania can be further improved with the design of efficient synthesis methodologies.

13. Opportunities, Challenges and Future Prospects

Titanium dioxide has a wide range of properties associated to it; it is a semiconductor [227] with varied properties such as being non-toxic [228], highly efficient [229], cost-effective [230], highly reactive [231], and eco-friendly. It has been accepted globally as a photocatalyst because of its high pore size [232], notable band gap [233], and large surface area [234]. Nevertheless, it has certain drawbacks, of which the following are related: the rejoining of the photo-generated charge bearers, low adsorption range, and the ineffectual visible-light utilization which requires improvement for the intensified photocatalytic activity. Numerous researchers have been regulated to undermine the limitations related to the photocatalysis of titania; the incorporation of nanoparticles and the doping of metals and non-metals have helped in enhancing its process to a larger extent. The amalgamation of NPs has been of utmost importance lately because they produce the desired results by amending the particle shape and size along with the physicochemical properties of TiO_2. Moreover, doping can strengthen the photocatalytic property by minimizing the reposting of charge carriers and decreasing the band-shift towards the region of visible light.

The photooxidation of organic effluent in wastewater and the elimination of nitrates and sulfates, along with acidic, basic, VAT, and azo dyes, can be achieved by the non-metallic doping of TiO_2. Moreover, the sensitization of dyes can be achieved by the doping of non-metals with titania; it can help in the breakdown of pesticides, the industrial discharge of dyes which have toxic and malignant effects, and the generation of photocatalytic hydrogen [235].

It is important to understand the prospects and future aspects on improving the photocatalytic activity of TiO_2 by different means, either by doping or co-doping. The studies have shown that both manifest remarkable results. The subject of high noticeability here is that whose process has produced more beneficial and long-lasting outcomes. More studies focusing on the engineered edges via doping for the improvement of the conduction and valence bands are required for enhancement of the absorption band of titania. Furthermore, the movability of charge carriers should be increased by introducing an impurity to improve the working efficiency of TiO_2. Therefore, the use of photocatalysis along with some other technologies would improve its application, which would benefit the environment for a longer period.

Moreover, a gradual deactivation of the photocatalytic materials concerns all the potential industrial applications. A periodical regeneration of the photocatalytic materials would be required, which would also increase the overall cost. Therefore, cost would obviously remain an essential issue for commercialization. Hence, to overcome this obstacle, extensive research would be necessary to develop both economical reactors and photocatalytic materials. Concomitant, concerted, and extensive research progress to achieve these goals is necessary for the practical implementation of this technology.

Author Contributions: Conceptualization, P.A. and M.H.; methodology, A.A.; software, A.S.; validation, A.A.; A.S.; formal analysis, A.A.; investigation, P.A.; resources, M.H.; data curation, A.A.; writing—original draft preparation, P.A.; writing—review and editing, M.H.; visualization, P.A.; supervision, P.A.; project administration, P.A.; funding acquisition, M.H. All authors have read and agreed to the published version of the manuscript.

Funding: This research received no external funding.

Conflicts of Interest: The authors declare no conflict of interest.

References

1. Lee, K.M.; Lai, C.W.; Ngai, K.S.; Juan, J.C. Recent developments of zinc oxide based photocatalyst in water treatment technology: A review. *Water Res.* **2016**, *88*, 428–448. [CrossRef] [PubMed]
2. Etman, A.S.; Abdelhamid, H.N.; Yuan, Y.; Wang, L.; Zou, X.; Sun, J. Facile Water-Based Strategy for Synthesizing MoO_{3-x} Nanosheets: Efficient Visible Light Photocatalysts for Dye Degradation. *ACS Omega* **2018**, *3*, 2193–2201. [CrossRef] [PubMed]
3. Mittal, A.; Mittal, A.; Mari, B.; Sharma, S.; Kumari, V.; Maken, S.; Kumari, K.; Kumar, N. Non-metal modified TiO_2: A step towards visible light photocatalysis. *J. Mater. Sci. Mater. Electron.* **2019**, *30*, 3186–3207. [CrossRef]

4. Din, M.I.; Khalid, R.; Hussain, Z. Recent Research on Development and Modification of Nontoxic Semiconductor for Environmental Application. *Sep. Purif. Rev.* **2021**, *50*, 244–261. [CrossRef]
5. Al-Mamun, M.R.; Kader, S.; Islam, M.S.; Khan, M.Z.H. Photocatalytic activity improvement and application of UV-TiO_2 photocatalysis in textile wastewater treatment: A review. *J. Environ. Chem. Eng.* **2019**, *7*, 103248. [CrossRef]
6. Zhu, Z.; Kao, C.T.; Tang, B.H.; Chang, W.C.; Wu, R.J. Efficient hydrogen production by photocatalytic water-splitting using Pt-doped TiO_2 hollow spheres under visible light. *Ceram. Int.* **2016**, *42*, 6749–6754. [CrossRef]
7. Makama, A.B.; Salmiaton, A.; Saion, E.B.; Choong, T.S.Y.; Abdullah, N. Synthesis of CdS Sensitized TiO_2 Photocatalysts: Methylene Blue Adsorption and Enhanced Photocatalytic Activities. *Int. J. Photoenergy* **2016**, *2016*, 2947510. [CrossRef]
8. Huang, M.; Yu, S.; Li, B.; Lihui, D.; Zhang, F.; Fan, M.; Deng, C. Influence of preparation methods on the structure and catalytic performance of SnO_2-doped TiO_2 photocatalysts. *Ceram. Int.* **2014**, *40*, 13305–13312. [CrossRef]
9. Hassan, S.M.; Ahmed, A.I.; Mannaa, M.A. Preparation and characterization of SnO_2 doped TiO_2 nanoparticles: Effect of phase changes on the photocatalytic and catalytic activity. *J. Sci. Adv. Mater. Devices* **2019**, *4*, 400–412. [CrossRef]
10. Dontsova, T.A.; Kutuzova, A.S.; Bila, K.O.; Kyrii, S.O.; Kosogina, I.V.; Nechyporuk, D.O. Enhanced Photocatalytic Activity of TiO_2/SnO_2 Binary Nanocomposites. *J. Nanomater.* **2020**, *2020*, 8349480. [CrossRef]
11. Wang, X.; Sun, M.; Murugananthan, M.; Zhang, Y.; Zhang, L. Electrochemically self-doped WO_3/TiO_2 nanotubes for photocatalytic degradation of volatile organic compounds. *Appl. Catal. B Environ.* **2020**, *260*, 118205. [CrossRef]
12. Amouhadi, E.; Aliyan, H.; Aghaei, H.; Fazaeli, R.; Richeson, D. Photodegradation and mineralization of metronidazole by a novel quadripartite SnO_2@$TiO_2/ZrTiO_4/ZrO_2$ photocatalyst: Comprehensive photocatalyst characterization and kinetic study. *Mater. Sci. Semicond. Process.* **2022**, *143*, 106560. [CrossRef]
13. Liu, C.; Li, X.; Wu, Y.; Sun, L.; Zhang, L.; Chang, X.; Wang, X. Enhanced photocatalytic activity by tailoring the interface in TiO_2–$ZrTiO_4$ heterostructure in TiO_2–$ZrTiO_4$–SiO_2 ternary system. *Ceram. Int.* **2019**, *45*, 17163–17172. [CrossRef]
14. Liu, C.; Li, X.; Wu, Y.; Zhang, L.; Chang, X.; Yuan, X.; Wang, X. Fabrication of multilayer porous structured TiO_2–$ZrTiO_4$–SiO_2 heterostructure towards enhanced photo-degradation activities. *Ceram. Int.* **2020**, *46*, 476–486. [CrossRef]
15. Xiang, Q.; Yu, J.; Jaroniec, M. Graphene-based semiconductor photocatalysts. *Chem. Soc. Rev.* **2012**, *41*, 782–796. [CrossRef]
16. Rommozzi, E.; Zannotti, M.; Giovannetti, R.; D'Amato, C.A.; Ferraro, S.; Minicucci, M.; Di Cicco, A. Reduced Graphene Oxide/TiO_2 Nanocomposite: From Synthesis to Characterization for Efficient Visible Light Photocatalytic Applications. *Catalysts* **2018**, *8*, 598. [CrossRef]
17. Rahman, M.M.; Choudhury, F.A.; Hossain, D.; Chowdhury, N.I.; Mohsin, S.; Hasan, M.; Uddin, F.; Sarker, N.C. A Comparative study on the photocatalytic degradation of industrial dyes using modified commercial and synthesized TiO_2 photocatalysts. *J. Chem. Eng.* **2014**, *27*, 65–71. [CrossRef]
18. Shehzad, N.; Tahir, M.; Johari, K.; Murugesan, T.; Hussain, M.A. Critical review on TiO_2 based photocatalytic CO_2 reduction system: Strategies to improve efficiency. *J. CO_2 Util.* **2018**, *26*, 98–122. [CrossRef]
19. Hussain, M.; Ceccarelli, R.; Marchisio, D.L.; Fino, D.; Russo, N.; Geobaldo, F. Synthesis, characterization, and photocatalytic application of novel TiO_2 nanoparticles. *Chem. Eng. J.* **2010**, *157*, 45–51. [CrossRef]
20. Siraj, Z.; Maafa, I.M.; Shafiq, I.; Shezad, N.; Akhter, P.; Yang, W.; Hussain, M. KIT-6 induced mesostructured TiO_2 for photocatalytic degradation of methyl blue. *Environ. Sci. Pollut. Res.* **2021**, *28*, 53340–53352. [CrossRef]
21. Rashid, R.; Shafiq, I.; Iqbal, M.J.; Shabir, M.; Akhter, P.; Hamayun, M.H.; Hussain, M. Synergistic effect of NS co-doped TiO_2 adsorbent for removal of cationic dyes. *J. Environ. Chem. Eng.* **2021**, *9*, 105480. [CrossRef]
22. Hlekelele, L.; Durbach, S.H.; Chauke, V.P.; Dziike, F.; Franklyn, P.J. Resin-gel incorporation of high concentrations of W^{6+} and Zn^{2+} into TiO_2-anatase crystal to form quaternary mixed-metal oxides: Effect on the a lattice parameter and photodegradation efficiency. *RSC Adv.* **2019**, *9*, 36875–36883. [CrossRef] [PubMed]
23. Thambiliyagodage, C. Activity enhanced TiO_2 nanomaterials for photodegradation of dyes—A review. *Environ. Nanotechnol. Monit. Manag.* **2021**, *16*, 100592. [CrossRef]
24. Tryba, B.; Piszcz, M.; Morawski, A.W. Photocatalytic activity of-composites. *Int. J. Photoenergy* **2009**, *2009*, 297319. [CrossRef]
25. Han, F.; Kambala, V.S.R.; Srinivasan, M.; Rajarathnam, D.; Naidu, R. Tailored titanium dioxide photocatalysts for the degradation of organic dyes in wastewater treatment: A review. *Appl. Catal. A Gen.* **2009**, *359*, 25–40. [CrossRef]
26. Pragati, T.; Roshan, K.N. Synthesis of sol-gel derived TiO_2 nanoparticles for the photocatalytic degradation of methyl orange dye. *Res. J. Chem. Environ.* **2011**, *15*, 145–149.
27. Deng, H.; He, H.; Sun, S.; Zhu, X.; Zhou, D.; Han, F.; Pan, X. Photocatalytic degradation of dye by Ag/TiO_2 nanoparticles prepared with different sol–gel crystallization in the presence of effluent organic matter. *Environ. Sci. Pollut. Res.* **2019**, *26*, 35900–35912. [CrossRef]
28. Al Jitan, S.; Palmisano, G.; Garlisi, C. Synthesis and surface modification of TiO_2-based photocatalysts for the conversion of CO_2. *Catalysts* **2020**, *10*, 227. [CrossRef]
29. Islam, S.Z.; Nagpure, S.; Kim, D.Y.; Rankin, S.E. Synthesis and Catalytic Applications of Non-Metal Doped Mesoporous Titania. *Inorganics* **2017**, *5*, 15. [CrossRef]
30. Wu, Y.; Xing, M.; Tian, B.; Zhang, J.; Chen, F. Preparation of nitrogen and fluorine co-doped mesoporous TiO_2 microsphere and photodegradation of acid orange 7 under visible light. *Chem. Eng. J.* **2010**, *162*, 710–717. [CrossRef]
31. Yang, J.; Zhang, X.; Li, B.; Liu, H.; Sun, P.; Wang, C.; Liu, Y. Photocatalytic activities of heterostructured TiO_2-graphene porous microspheres prepared by ultrasonic spray pyrolysis. *J. Alloys Compd.* **2014**, *584*, 180–184. [CrossRef]

32. Zhou, X.; Peng, F.; Wang, H.; Yu, H.; Yang, J. Effect of nitrogen-doping temperature on the structure and photocatalytic activity of the B, N-doped TiO_2. *J. Solid State Chem.* **2011**, *184*, 134–140. [CrossRef]
33. El-Sheikh, S.M.; Zhang, G.; El-Hosainy, H.M.; Ismail, A.A.; O'Shea, K.E.; Falaras, P.; Dionysiou, D.D. High performance sulfur, nitrogen and carbon doped mesoporous anatase–brookite TiO_2 photocatalyst for the removal of microcystin-LR under visible light irradiation. *J. Hazard. Mater.* **2014**, *280*, 723–733. [CrossRef]
34. Ao, Y.; Xu, J.; Fu, D.; Yuan, C. Synthesis of C, N, S-tridoped mesoporous titania with enhanced visible light-induced photocatalytic activity. *Microporous Mesoporous Mater.* **2009**, *122*, 1–6. [CrossRef]
35. Almaev, A.V.; Yakovlev, N.N.; Kushnarev, B.O.; Kopyev, V.V.; Novikov, V.A.; Zinoviev, M.M.; Yudin, N.N.; Podzivalov, S.N.; Erzakova, N.N.; Chikiryaka, A.V.; et al. Gas Sensitivity of IBSD Deposited TiO_2 Thin Films. *Coatings* **2022**, *12*, 1565. [CrossRef]
36. Mele, G.; del Sole, R.; Lü, X. 18—Applications of TiO_2 in sensor devices. In *Titanium Dioxide (TiO_2) and Its Applications*; Parrino, F., Palmisano, L., Eds.; Elsevier: Amsterdam, The Netherlands, 2021; pp. 527–581.
37. Gogova, D.; Iossifova, A.; Ivanova, T.; Dimitrova, Z.; Gesheva, K. Electrochromic behavior in CVD grown tungsten oxide films. *J. Cryst. Growth* **1999**, *198–199*, 1230–1234. [CrossRef]
38. Fan, X.; Chen, X.; Zhu, S.; Li, Z.; Yu, T.; Ye, J.; Zou, Z. The structural, physical and photocatalytic properties of the mesoporous Cr-doped TiO_2. *J. Mol. Catal. A Chem.* **2008**, *284*, 155–160. [CrossRef]
39. Murthy, N.S. Scattering techniques for structural analysis of biomaterials. In *Characterization of Biomaterials*; Elsevier: Amsterdam, The Netherlands, 2013; pp. 34–72.
40. Ghumro, S.S.; Lal, B.; Pirzada, T. Visible-Light-Driven Carbon-Doped TiO_2-Based Nanocatalysts for Enhanced Activity toward Microbes and Removal of Dye. *ACS Omega* **2022**, *7*, 4333–4341. [CrossRef]
41. Negi, C.; Kandwal, P.; Rawat, J.; Sharma, M.; Sharma, H.; Dalapati, G.; Dwivedi, C. Carbon-doped titanium dioxide nanoparticles for visible light driven photocatalytic activity. *Appl. Surf. Sci.* **2021**, *554*, 149553. [CrossRef]
42. Piątkowska, A.; Janus, M.; Szymański, K.; Mozia, S. C-, N- and S-Doped TiO_2 Photocatalysts: A Review. *Catalysts* **2021**, *11*, 144. [CrossRef]
43. Bergamonti, L.; Predieri, G.; Paz, Y.; Fornasini, L.; Lottici, P.P.; Bondioli, F. Enhanced self-cleaning properties of N-doped TiO_2 coating for Cultural Heritage. *Microchem. J.* **2017**, *133*, 1–12. [CrossRef]
44. Chen, X.; Kuo, D.-H.; Lu, D. N-doped mesoporous TiO_2 nanoparticles synthesized by using biological renewable nanocrystalline cellulose as template for the degradation of pollutants under visible and sun light. *Chem. Eng. J.* **2016**, *295*, 192–200. [CrossRef]
45. Hwang, Y.J.; Yang, S.; Lee, H. Surface analysis of N-doped TiO_2 nanorods and their enhanced photocatalytic oxidation activity. *Appl. Catal. B Environ.* **2017**, *204*, 209–215. [CrossRef]
46. Chung, K.-H.; Kim, B.J.; Park, Y.K.; Kim, S.C.; Jung, S.C. Photocatalytic Properties of Amorphous N-Doped TiO_2 Photocatalyst under Visible Light Irradiation. *Catalysts* **2021**, *11*, 1010. [CrossRef]
47. Shabir, M.; Shezad, N.; Shafiq, I.; Maafa, I.M.; Akhter, P.; Azam, K.; Hussain, M. Carbon nanotubes loaded N, S-codoped TiO_2: Heterojunction assembly for enhanced integrated adsorptive-photocatalytic performance. *J. Ind. Eng. Chem.* **2022**, *105*, 539–548. [CrossRef]
48. Li, T.; Abdelhaleem, A.; Chu, W.; Pu, S.; Qi, F.; Zou, J. S-doped TiO_2 photocatalyst for visible LED mediated oxone activation: Kinetics and mechanism study for the photocatalytic degradation of pyrimethanil fungicide. *Chem. Eng. J.* **2021**, *411*, 128450. [CrossRef]
49. Grabowska, E.; Zaleska, A.; Sobczak, J.W.; Gazda, M.; Hupka, J. Boron-doped TiO_2: Characteristics and photoactivity under visible light. *Procedia Chem.* **2009**, *1*, 1553–1559. [CrossRef]
50. Koli, V.B.; Ke, S.-C.; Dodamani, A.G.; Deshmukh, S.P.; Kim, J.-S. Boron-Doped TiO_2-CNT Nanocomposites with Improved Photocatalytic Efficiency toward Photodegradation of Toluene Gas and Photo-Inactivation of Escherichia coli. *Catalysts* **2020**, *10*, 632. [CrossRef]
51. Su, Y.; Xiao, Y.; Fu, X.; Deng, Y.; Zhang, F. Photocatalytic properties and electronic structures of iodine-doped TiO_2 nanotubes. *Mater. Res. Bull.* **2009**, *44*, 2169–2173. [CrossRef]
52. Xu, J.; Yang, B.; Wu, M.; Fu, Z.; Lv, Y.; Zhao, Y. Novel N−F-Codoped TiO_2 Inverse Opal with a Hierarchical Meso-/Macroporous Structure: Synthesis, Characterization, and Photocatalysis. *J. Phys. Chem. C* **2010**, *114*, 15251–15259. [CrossRef]
53. Morales-Torres, S.; Pastrana-Martínez, L.M.; Figueiredo, J.L.; Faria, J.L.; Silva, A.M. Design of graphene-based TiO_2 photocatalysts—A review. *Environ. Sci. Pollut. Res.* **2012**, *19*, 3676–3687. [CrossRef]
54. Suárez, S.; Jansson, I.; Ohtani, B.; Sánchez, B. From titania nanoparticles to decahedral anatase particles: Photocatalytic activity of TiO_2/zeolite hybrids for VOCs oxidation. *Catal. Today* **2019**, *326*, 2–7. [CrossRef]
55. Liang, H.; Wang, Z.; Liao, L.; Chen, L.; Li, Z.; Feng, J. High performance photocatalysts: Montmorillonite supported-nano TiO_2 composites. *Optik* **2017**, *136*, 44–51. [CrossRef]
56. Shao, J.; Sheng, W.; Wang, M.; Li, S.; Chen, J.; Zhang, Y.; Cao, S. In situ synthesis of carbon-doped TiO_2 single-crystal nanorods with a remarkably photocatalytic efficiency. *Appl. Catal. B Environ.* **2017**, *209*, 311–319. [CrossRef]
57. Saiful Amran, S.N.B.; Wongso, V.; Abdul Halim, N.S.; Husni, M.K.; Sambudi, N.S.; Wirzal, M.D.H. Immobilized carbon-doped TiO_2 in polyamide fibers for the degradation of methylene blue. *J. Asian Ceram. Soc.* **2019**, *7*, 321–330. [CrossRef]
58. Habibi, S.; Jamshidi, M. Sol–gel synthesis of carbon-doped TiO_2 nanoparticles based on microcrystalline cellulose for efficient photocatalytic degradation of methylene blue under visible light. *Environ. Technol.* **2020**, *41*, 3233–3247. [CrossRef]

59. Ji, L.; Liu, X.; Xu, T.; Gong, M.; Zhou, S. Preparation and photocatalytic properties of carbon/carbon-doped TiO_2 double-layer hollow microspheres. *J. Sol-Gel Sci. Technol.* **2020**, *93*, 380–390. [CrossRef]
60. Bhosale, R.R.; Pujari, S.R.; Muley, G.G.; Patil, S.H.; Patil, K.R.; Shaikh, M.F.; Gambhire, A.B. Solar photocatalytic degradation of methylene blue using doped TiO_2 nanoparticles. *J. Sol. Energy.* **2014**, *103*, 473–479. [CrossRef]
61. Cong, Y.; Zhang, J.; Chen, F.; Anpo, M. Synthesis and Characterization of Nitrogen-Doped TiO_2 Nanophotocatalyst with High Visible Light Activity. *J. Phys. Chem. C* **2007**, *111*, 6976–6982. [CrossRef]
62. Senthilnathan, J.; Philip, L. Photocatalytic degradation of lindane under UV and visible light using N-doped TiO_2. *Chem. Eng. J.* **2010**, *161*, 83–92. [CrossRef]
63. Liu, X.; Chen, Y.; Cao, C.; Xu, J.; Qian, Q.; Luo, Y.; Chen, Q. Electrospun nitrogen and carbon co-doped porous TiO_2 nanofibers with high visible light photocatalytic activity. *N. J. Chem.* **2015**, *39*, 6944–6950. [CrossRef]
64. Pu, X.; Hu, Y.; Cui, S.; Cheng, L.; Jiao, Z. Preparation of N-doped and oxygen-deficient TiO_2 microspheres via a novel electron beam-assisted method. *Solid State Sci.* **2017**, *70*, 66–73. [CrossRef]
65. Panghulan, G.R.; Vasquez Jr, M.R.; Edañol, Y.D.; Chanlek, N.; Payawan Jr, L.M. Synthesis of TiN/N-doped TiO_2 composite films as visible light active photocatalyst. *J. Vac. Sci. Technol. B* **2020**, *38*, 062203. [CrossRef]
66. Ji, L.; Zhou, S.; Liu, X.; Gong, M.; Xu, T. Synthesis of carbon- and nitrogen-doped TiO_2/carbon composite fibers by a surface-hydrolyzed PAN fiber and their photocatalytic property. *J. Mater. Sci.* **2020**, *55*, 2471–2481. [CrossRef]
67. Divyasri, Y.V.; Reddy, N.L.; Lee, K.; Sakar, M.; Rao, V.N.; Venkatramu, V.; Reddy, N.C. GOptimization of N doping in TiO_2 nanotubes for the enhanced solar light mediated photocatalytic H_2 production and dye degradation. *Environ. Pollut.* **2021**, *269*, 116170. [CrossRef]
68. Tian, H.; Ma, J.; Li, K.; Li, J. Hydrothermal synthesis of S-doped TiO_2 nanoparticles and their photocatalytic ability for degradation of methyl orange. *Ceram. Int.* **2009**, *35*, 1289–1292. [CrossRef]
69. Birben, N.C.; Uyguner-Demirel, C.S.; Sen-Kavurmaci, S.; Gurkan, Y.Y.; Turkten, N.; Cinar, Z.; Bekbolet, M. Comparative evaluation of anion doped photocatalysts on the mineralization and decolorization of natural organic matter. *Catal. Today* **2015**, *240*, 125–131. [CrossRef]
70. Syafiuddin, A.; Hadibarata, T.; Zon, N.F. Characterization of Titanium Dioxide Doped with Nitrogen and Sulfur and Its Photocatalytic Appraisal for Degradation of Phenol and Methylene Blue. *J. Chin. Chem. Soc.* **2017**, *64*, 1333–1339. [CrossRef]
71. Gao, H.-T.; Liu, Y.Y.; Ding, C.H.; Dai, D.M.; Liu, G.J. Synthesis, characterization, and theoretical study of N, S-codoped nano-TiO_2 with photocatalytic activities. *Int. J. Miner. Metall. Mater.* **2011**, *18*, 606. [CrossRef]
72. Raj, K.J.A.; Ramaswamy, A.; Viswanathan, B. Surface area, pore size, and particle size engineering of titania with seeding technique and phosphate modification. *J. Phys. Chem. C* **2009**, *113*, 13750–13757. [CrossRef]
73. Ghafoor, S.; Aftab, F.; Rauf, A.; Duran, H.; Kirchhoff, K.; Arshad, S.N. P-doped TiO_2 Nanofibers Decorated with Ag Nanoparticles for Enhanced Photocatalytic Activity under Simulated Solar Light. *ChemistrySelect* **2020**, *5*, 14078–14085. [CrossRef]
74. Sarker, D.R.; Uddin, M.N.; Elias, M.; Rahman, Z.; Paul, R.K.; Siddiquey, I.A.; Uddin, J. P-doped TiO_2-MWCNTs nanocomposite thin films with enhanced photocatalytic activity under visible light exposure. *Clean. Eng. Technol.* **2022**, *6*, 100364. [CrossRef]
75. Xiao, J.; Pan, Z.; Zhang, B.; Liu, G.; Zhang, H.; Song, X.; Zheng, Y. The research of photocatalytic activity on Si doped TiO_2 nanotubes. *Mater. Lett.* **2017**, *188*, 66–68. [CrossRef]
76. Ajmal, A.; Majeed, I.; Malik, R.N.; Idriss, H.; Nadeem, M.A. Principles and mechanisms of photocatalytic dye degradation on TiO_2 based photocatalysts: A comparative overview. *RSC Adv.* **2014**, *4*, 37003–37026. [CrossRef]
77. O'Neill, C.; Hawkes, F.R.; Hawkes, D.L.; Lourenço, N.D.; Pinheiro, H.M.; Delée, W. Colour in textile effluents–sources, measurement, discharge consents and simulation: A review. *J. Chem. Technol. Biotechnol. Int. Res. Process Environ. Clean Technol.* **1999**, *74*, 1009–1018. [CrossRef]
78. Tehrani-Bagha, A.; Mahmoodi, N.M.; Menger, F. Degradation of a persistent organic dye from colored textile wastewater by ozonation. *Desalination* **2010**, *260*, 34–38. [CrossRef]
79. Andriantsiferana, C.; Mohamed, E.F.; Delmas, H. Photocatalytic degradation of an azo-dye on TiO_2/activated carbon composite material. *Environ. Technol.* **2014**, *35*, 355–363. [CrossRef]
80. Gao, Y.; Yang, B.; Wang, Q. Biodegradation and decolorization of dye wastewater: A review. In *IOP Conference Series: Earth and Environmental Science*; IOP Publishing: Bristol, UK, 2018.
81. Reza, K.M.; Kurny, A.; Gulshan, F. Parameters affecting the photocatalytic degradation of dyes using TiO_2: A review. *Appl. Water Sci.* **2017**, *7*, 1569–1578. [CrossRef]
82. Madhavan, J.; Maruthamuthu, P.; Murugesan, S.; Anandan, S. Kinetic studies on visible light-assisted degradation of acid red 88 in presence of metal-ion coupled oxone reagent. *Appl. Catal. B Environ.* **2008**, *83*, 8–14. [CrossRef]
83. Baran, W.; Makowski, A.; Wardas, W. The influence of $FeCl_3$ on the photocatalytic degradation of dissolved azo dyes in aqueous TiO_2 suspensions. *Chemosphere* **2003**, *53*, 87–95. [CrossRef]
84. Rauf, M.; Meetani, M.; Hisaindee, S. An overview on the photocatalytic degradation of azo dyes in the presence of TiO_2 doped with selective transition metals. *Desalination* **2011**, *276*, 13–27. [CrossRef]
85. Zhang, T.; ki Oyama, T.; Horikoshi, S.; Hidaka, H.; Zhao, J.; Serpone, N. Photocatalyzed N-demethylation and degradation of methylene blue in titania dispersions exposed to concentrated sunlight. *Sol. Energy Mater. Sol. Cells* **2002**, *73*, 287–303. [CrossRef]
86. Suteu, D.; Malutan, T. Industrial cellolignin wastes as adsorbent for removal of methylene blue dye from aqueous solutions. *BioResources* **2013**, *8*, 427–446. [CrossRef]

87. Christie, R. *Carbonyl Dyes and Pigments*; RSC Publishing: London, UK, 2001.
88. Thung, W.-E.; Ong, S.A.; Ho, L.N.; Wong, Y.S.; Ridwan, F.; Oon, Y.L.; Lehl, H.K. A highly efficient single chambered up-flow membrane-less microbial fuel cell for treatment of azo dye Acid Orange 7-containing wastewater. *Bioresour. Technol.* **2015**, *197*, 284–288. [CrossRef] [PubMed]
89. Houas, A.; Lachheb, H.; Ksibi, M.; Elaloui, E.; Guillard, C.; Herrmann, J.M. Photocatalytic degradation pathway of methylene blue in water. *Appl. Catal. B Environ.* **2001**, *31*, 145–157. [CrossRef]
90. Konstantinou, I.K.; Albanis, T.A. TiO_2-assisted photocatalytic degradation of azo dyes in aqueous solution: Kinetic and mechanistic investigations: A review. *Appl. Catal. B Environ.* **2004**, *49*, 1–14. [CrossRef]
91. Anwer, H.; Mahmood, A.; Lee, J.; Kim, K.H.; Park, J.W.; Yip, A.C. Photocatalysts for degradation of dyes in industrial effluents: Opportunities and challenges. *Nano Res.* **2019**, *12*, 955–972. [CrossRef]
92. Chu, C.-Y.; Huang, M.H. Facet-dependent photocatalytic properties of Cu_2O crystals probed by using electron, hole and radical scavengers. *J. Mater. Chem. A* **2017**, *5*, 15116–15123. [CrossRef]
93. Meng, L.; Chen, Z.; Ma, Z.; He, S.; Hou, Y.; Li, H.H.; Long, J. Gold plasmon-induced photocatalytic dehydrogenative coupling of methane to ethane on polar oxide surfaces. *Energy Environ. Sci.* **2018**, *11*, 294–298. [CrossRef]
94. Wang, S.; Boyjoo, Y.; Choueib, A. A comparative study of dye removal using fly ash treated by different methods. *Chemosphere* **2005**, *60*, 1401–1407. [CrossRef]
95. Katheresan, V.; Kansedo, J.; Lau, S.Y. Efficiency of various recent wastewater dye removal methods: A review. *J. Environ. Chem. Eng.* **2018**, *6*, 4676–4697. [CrossRef]
96. Mondal, S. Methods of Dye Removal from Dye House Effluent—An Overview. *Environ. Eng. Sci.* **2008**, *25*, 383–396. [CrossRef]
97. Kaykhaii, M.; Sasani, M.; Marghzari, S. Removal of dyes from the environment by adsorption process. *Chem. Mater. Eng.* **2018**, *6*, 31–35. [CrossRef]
98. Piaskowski, K.; Świderska-Dąbrowska, R.; Zarzycki, P.K. Dye Removal from Water and Wastewater Using Various Physical, Chemical, and Biological Processes. *J. AOAC Int.* **2019**, *101*, 1371–1384. [CrossRef]
99. El-Desouky, M.G.; El-Bindary, M.A.; El-Bindary, A.A. Effective adsorptive removal of anionic dyes from aqueous solution. *Vietnam J. Chem.* **2021**, *59*, 341–361.
100. Alhujaily, A.; Yu, H.; Zhang, X.; Ma, F. Adsorptive removal of anionic dyes from aqueous solutions using spent mushroom waste. *Appl. Water Sci.* **2020**, *10*, 183. [CrossRef]
101. Pavithra, K.G.; Jaikumar, V. Removal of colorants from wastewater: A review on sources and treatment strategies. *J. Ind. Eng. Chem.* **2019**, *75*, 1–19. [CrossRef]
102. Zhao, X.; Wang, X.; Lou, T. Simultaneous adsorption for cationic and anionic dyes using chitosan/electrospun sodium alginate nanofiber composite sponges. *Carbohydr. Polym.* **2022**, *276*, 118728. [CrossRef]
103. Mallakpour, S.; Rashidimoghadam, S. 9—Carbon nanotubes for dyes removal. In *Composite Nanoadsorbents*; Kyzas, G.Z., Mitropoulos, A.C., Eds.; Elsevier: Amsterdam, The Netherlands, 2019; pp. 211–243.
104. Velusamy, S.; Roy, A.; Sundaram, S.; Kumar Mallick, T. A Review on Heavy Metal Ions and Containing Dyes Removal through Graphene Oxide-Based Adsorption Strategies for Textile Wastewater Treatment. *Chem. Rec.* **2021**, *21*, 1570–1610. [CrossRef]
105. Ling, C.; Yimin, D.; Qi, L.; Chengqian, F.; Zhiheng, W.; Yaqi, L.; Li, W. Novel High-efficiency adsorbent consisting of magnetic Cellulose-based ionic liquid for removal of anionic dyes. *J. Mol. Liq.* **2022**, *353*, 118723. [CrossRef]
106. Rahman, F.; Akter, M. Removal of dyes form textile wastewater by adsorption using shrimp shell. *Int. J. Waste Resour.* **2016**, *6*, 2–5.
107. Ledakowicz, S.; Paździor, K. Recent Achievements in Dyes Removal Focused on Advanced Oxidation Processes Integrated with Biological Methods. *Molecules* **2021**, *26*, 870. [CrossRef] [PubMed]
108. Bal, G.; Thakur, A. Distinct approaches of removal of dyes from wastewater: A review. *Mater. Today Proc.* **2022**, *50*, 1575–1579. [CrossRef]
109. Raval, N.P.; Shah, P.U.; Shah, N.K. Malachite green "a cationic dye" and its removal from aqueous solution by adsorption. *Appl. Water Sci.* **2017**, *7*, 3407–3445. [CrossRef]
110. Ruan, W.; Hu, J.; Qi, J.; Hou, Y.; Zhou, C.; Wei, X. Removal of dyes from wastewater by nanomaterials: A review. *Adv. Mater. Lett.* **2019**, *10*, 9–20. [CrossRef]
111. Sleiman, M.; Vildozo, D.; Ferronato, C.; Chovelon, J.M. Photocatalytic degradation of azo dye Metanil Yellow: Optimization and kinetic modeling using a chemometric approach. *Appl. Catal. B Environ.* **2007**, *77*, 1–11. [CrossRef]
112. Basavarajappa, P.S.; Patil, S.B.; Ganganagappa, N.; Reddy, K.R.; Raghu, A.V.; Reddy, C. Recent progress in metal-doped TiO_2, non-metal doped/codoped TiO_2 and TiO_2 nanostructured hybrids for enhanced photocatalysis. *Int. J. Hydrog. Energy* **2020**, *45*, 7764–7778. [CrossRef]
113. Guo, W.; Wu, L.; Chen, Z.; Boschloo, G.; Hagfeldt, A.; Ma, T. Highly efficient dye-sensitized solar cells based on nitrogen-doped titania with excellent stability. *J. Photochem. Photobiol. A Chem.* **2011**, *219*, 180–187. [CrossRef]
114. Wu, Y.; Xing, M.; Zhang, J. Gel-hydrothermal synthesis of carbon and boron co-doped TiO_2 and evaluating its photocatalytic activity. *J. Hazard. Mater.* **2011**, *192*, 368–373. [CrossRef]
115. Boikanyo, D.; Masheane, M.L.; Nthunya, L.N.; Mishra, S.B.; Mhlanga, S.D. Carbon-supported photocatalysts for organic dye photodegradation. In *New Polymer Nanocomposites for Environmental Remediation*; Elsevier: Amsterdam, The Netherlands, 2018; pp. 99–138.

116. Liu, J.; Zhu, W.; Yu, S.; Yan, X. Three dimensional carbogenic dots/TiO2 nanoheterojunctions with enhanced visible light-driven photocatalytic activity. *Carbon* **2014**, *79*, 369–379. [CrossRef]
117. Matos, J.; Miralles-Cuevas, S.; Ruíz-Delgado, A.; Oller, I.; Malato, S. Development of TiO_2-C photocatalysts for solar treatment of polluted water. *Carbon* **2017**, *122*, 361–373. [CrossRef]
118. Shi, Z.-J.; Ma, M.-G.; Zhu, J.-F. Recent Development of Photocatalysts Containing Carbon Species: A Review. *Catalysts* **2018**, *9*, 20. [CrossRef]
119. Noorimotlagh, Z.; Kazeminezhad, I.; Jaafarzadeh, N.; Ahmadi, M.; Ramezani, Z.; Martinez, S.S. The visible-light photodegradation of nonylphenol in the presence of carbon-doped TiO_2 with rutile/anatase ratio coated on GAC: Effect of parameters and degradation mechanism. *J. Hazard. Mater.* **2018**, *350*, 108–120. [CrossRef]
120. Shaban, Y.A.; El Maradny, A.A.; Al Farawati, R.K. Photocatalytic reduction of nitrate in seawater using C/TiO_2 nanoparticles. *J. Photochem. Photobiol. A Chem.* **2016**, *328*, 114–121. [CrossRef]
121. Ananpattarachai, J.; Seraphin, S.; Kajitvichyanukul, P. Formation of hydroxyl radicals and kinetic study of 2-chlorophenol photocatalytic oxidation using C-doped TiO_2, N-doped TiO_2, and C, N Co-doped TiO_2 under visible light. *Environ. Sci. Pollut. Res.* **2016**, *23*, 3884–3896. [CrossRef]
122. Rajamanickam, A.; Thirunavukkarasu, P.; Dhanakodi, K. A simple route to synthesis of carbon doped TiO_2 nanostructured thin film for enhanced visible-light photocatalytic activity. *J. Mater. Sci. Mater. Electron.* **2015**, *26*, 4038–4045. [CrossRef]
123. Shi, J.-W.; Liu, C.; He, C.; Li, J.; Xie, C.; Yang, S.; Chen, J.-W.; Li, S.; Niu, C. Carbon-doped titania nanoplates with exposed {001} facets: Facile synthesis, characterization and visible-light photocatalytic performance. *RSC Adv.* **2015**, *5*, 17667–17675. [CrossRef]
124. Shaban, Y.A.; Fallata, H.M. Sunlight-induced photocatalytic degradation of acetaminophen over efficient carbon doped TiO_2 ($CTiO_2$) nanoparticles. *Res. Chem. Intermed.* **2019**, *45*, 2529–2547. [CrossRef]
125. De Luna, M.D.G.; Chun-Te Lin, J.; Gotostos, M.J.N.; Lu, M.C. Photocatalytic oxidation of acetaminophen using carbon self-doped titanium dioxide. *Sustain. Environ. Res.* **2016**, *26*, 161–167. [CrossRef]
126. Yuan, Y.; Qian, X.; Han, H.; Chen, Y. Synthesis of carbon modified TiO_2 photocatalysts with high photocatalytic activity by a facile calcinations assisted solvothermal method. *J. Mater. Sci. Mater. Electron.* **2017**, *28*, 10028–10034. [CrossRef]
127. Kuang, L.; Zhang, W. Enhanced hydrogen production by carbon-doped TiO_2 decorated with reduced graphene oxide (rGO) under visible light irradiation. *RSC Adv.* **2016**, *6*, 2479–2488. [CrossRef]
128. An, N.; Ma, Y.; Liu, J.; Ma, H.; Yang, J.; Zhang, Q. Enhanced visible-light photocatalytic oxidation capability of carbon-doped TiO_2 via coupling with fly ash. *Chin. J. Catal.* **2018**, *39*, 1890–1900. [CrossRef]
129. Zhang, J.; Huang, G.F.; Li, D.; Zhou, B.X.; Chang, S.; Pan, A.; Huang, W.Q. Facile route to fabricate carbon-doped TiO_2 nanoparticles and its mechanism of enhanced visible light photocatalytic activity. *Appl. Phys. A* **2016**, *122*, 994. [CrossRef]
130. Noorimotlagh, Z.; Kazeminezhad, I.; Jaafarzadeh, N.; Ahmadi, M.; Ramezani, Z. Improved performance of immobilized TiO_2 under visible light for the commercial surfactant degradation: Role of carbon doped $TiO_{60}$and anatase/rutile ratio. *Catal. Today* **2020**, *348*, 277–289. [CrossRef]
131. Saharudin, K.A.; Sreekantan, S.; Lai, C.W. Fabrication and photocatalysis of nanotubular C-doped TiO_2 arrays: Impact of annealing atmosphere on the degradation efficiency of methyl orange. *Mater. Sci. Semicond. Process.* **2014**, *20*, 1–6. [CrossRef]
132. Wang, X.; Lim, T.-T. Solvothermal synthesis of C–N codoped TiO_2 and photocatalytic evaluation for bisphenol A degradation using a visible-light irradiated LED photoreactor. *Appl. Catal. B Environ.* **2010**, *100*, 355–364. [CrossRef]
133. Wu, D.; Wang, L. Low-temperature synthesis of anatase C-N-TiO_2 photocatalyst with enhanced visible-light-induced photocatalytic activity. *Appl. Surf. Sci.* **2013**, *271*, 357–361. [CrossRef]
134. Wang, M.; Han, J.; Hu, Y.; Guo, R. Mesoporous C, N-codoped TiO_2 hybrid shells with enhanced visible light photocatalytic performance. *RSC Adv.* **2017**, *7*, 15513–15520. [CrossRef]
135. Zhang, X.; Zhang, Y.; Zhou, L.; Li, X.; Guo, X. In situ C,N-codoped mesoporous TiO_2 nanocrystallites with high surface areas and worm-like structure for efficient photocatalysis. *J. Porous Mater.* **2018**, *25*, 571–579. [CrossRef]
136. Ohtani, B. Photocatalysis A to Z—What we know and what we do not know in a scientific sense. *J. Photochem. Photobiol. C Photochem. Rev.* **2010**, *11*, 157–178. [CrossRef]
137. Song, L.; Jing, W.; Chen, J.; Zhang, S.; Zhu, Y.; Xiong, J. High reusability and durability of carbon-doped TiO_2/carbon nanofibrous film as visible-light-driven photocatalyst. *J. Mater. Sci.* **2019**, *54*, 3795–3804. [CrossRef]
138. Lavand, A.B.; Bhatu, M.N.; Malghe, Y.S. Visible light photocatalytic degradation of malachite green using modified titania. *J. Mater. Res. Technol.* **2019**, *8*, 299–308. [CrossRef]
139. Fang, Y.; Liu, Y.; Qi, L.; Xue, Y.; Li, Y. 2D graphdiyne: An emerging carbon material. *Chem. Soc. Rev.* **2022**, *51*, 2681–2709. [CrossRef]
140. Zheng, Z.; Xue, Y.; Li, Y. A new carbon allotrope: Graphdiyne. *Trends Chem.* **2022**, *4*, 754–768. [CrossRef]
141. Wang, W.; Chen, M.; Huang, D.; Zeng, G.; Zhang, C.; Lai, C.; Wang, Z. An overview on nitride and nitrogen-doped photocatalysts for energy and environmental applications. *Compos. Part B Eng.* **2019**, *172*, 704–723. [CrossRef]
142. Ansari, S.A.; Khan, M.M.; Ansari, M.O.; Cho, M.H. Nitrogen-doped titanium dioxide (N-doped TiO2) for visible light photocatalysis. *N. J. Chem.* **2016**, *40*, 3000–3009. [CrossRef]
143. Gomathi Devi, L.; Kavitha, R. Review on modified N–TiO_2 for green energy applications under UV/visible light: Selected results and reaction mechanisms. *RSC Adv.* **2014**, *4*, 28265–28299. [CrossRef]

144. Samokhvalov, A. Hydrogen by photocatalysis with nitrogen codoped titanium dioxide. *Renew. Sustain. Energy Rev.* **2017**, *72*, 981–1000. [CrossRef]
145. Peng, F.; Cai, L.; Yu, H.; Wang, H.; Yang, J. Synthesis and characterization of substitutional and interstitial nitrogen-doped titanium dioxides with visible light photocatalytic activity. *J. Solid State Chem.* **2008**, *181*, 130–136. [CrossRef]
146. Sacco, O.; Stoller, M.; Vaiano, V.; Ciambelli, P.; Chianese, A.; Sannino, D. Photocatalytic degradation of organic dyes under visible light on N-doped TiO_2 photocatalysts. *Int. J. Photoenergy* **2012**, *2012*, 626759. [CrossRef]
147. Thambiliyagodage, C.; Usgodaarachchi, L. Photocatalytic activity of N, Fe and Cu co-doped TiO_2 nanoparticles under sunlight. *Curr. Res. Green Sustain. Chem.* **2021**, *4*, 100186. [CrossRef]
148. Preethi, L.K.; Antony, R.P.; Mathews, T.; Walczak, L.; Gopinath, C.S. A study on doped heterojunctions in TiO_2 nanotubes: An efficient photocatalyst for solar water splitting. *Sci. Rep.* **2017**, *7*, 14314. [CrossRef] [PubMed]
149. Sirivallop, A.; Areerob, T.; Chiarakorn, S. Enhanced visible light photocatalytic activity of N and Ag doped and co-doped TiO_2 synthesized by using an in-situ solvothermal method for gas phase ammonia removal. *Catalysts* **2020**, *10*, 251. [CrossRef]
150. Xu, X.; Song, W. Enhanced H_2 production activity under solar irradiation over N-doped TiO_2 prepared using pyridine as a precursor: A typical sample of N-doped TiO_2 series. *Mater. Technol.* **2017**, *32*, 52–63. [CrossRef]
151. Ariza-Tarazona, M.C.; Villarreal-Chiu, J.F.; Barbieri, V.; Siligardi, C.; Cedillo-González, E.I. New strategy for microplastic degradation: Green photocatalysis using a protein-based porous N-TiO_2 semiconductor. *Ceram. Int.* **2019**, *45*, 9618–9624. [CrossRef]
152. Cheng, Z.-L.; Han, S. Preparation and photoelectrocatalytic performance of N-doped TiO_2/NaY zeolite membrane composite electrode material. *Water Sci. Technol.* **2016**, *73*, 486–492. [CrossRef]
153. Marques, J.; Gomes, T.D.; Forte, M.A.; Silva, R.F.; Tavares, C.J. A new route for the synthesis of highly-active N-doped TiO_2 nanoparticles for visible light photocatalysis using urea as nitrogen precursor. *Catal. Today* **2019**, *326*, 36–45. [CrossRef]
154. Cao, Y.; Xing, Z.; Shen, Y.; Li, Z.; Wu, X.; Yan, X.; Zhou, W. Mesoporous black Ti^{3+}/N-TiO_2 spheres for efficient visible-light-driven photocatalytic performance. *Chem. Eng. J.* **2017**, *325*, 199–207. [CrossRef]
155. Xing, X.; Du, Z.; Zhuang, J.; Wang, D. Removal of ciprofloxacin from water by nitrogen doped TiO_2 immobilized on glass spheres: Rapid screening of degradation products. *J. Photochem. Photobiol. A Chem.* **2018**, *359*, 23–32. [CrossRef]
156. Mohammadalipour, Z.; Rahmati, M.; Khataee, A.; Moosavi, M.A. Differential effects of N-TiO_2 nanoparticle and its photo-activated form on autophagy and necroptosis in human melanoma A375 cells. *J. Cell. Physiol.* **2020**, *235*, 8246–8259. [CrossRef]
157. Zangeneh, H.; Mousavi, S.A.; Eskandari, P. Comparison the visible photocatalytic activity and kinetic performance of amino acids (non-metal doped) TiO_2 for degradation of colored wastewater effluent. *Mater. Sci. Semicond. Process.* **2022**, *140*, 106383. [CrossRef]
158. Asahi, R.; Morikawa, T.; Ohwaki, T.; Aoki, K.; Taga, Y. Visible-light photocatalysis in nitrogen-doped titanium oxides. *Science* **2001**, *293*, 269–271. [CrossRef]
159. Umebayashi, T.; Yamaki, T.; Tanaka, S.; Asai, K. Visible light-induced degradation of methylene blue on S-doped TiO_2. *Chem. Lett.* **2003**, *32*, 330–331. [CrossRef]
160. Ho, W.; Jimmy, C.Y.; Lee, S. Low-temperature hydrothermal synthesis of S-doped TiO_2 with visible light photocatalytic activity. *J. Solid State Chem.* **2006**, *179*, 1171–1176. [CrossRef]
161. Niu, Y.; Xing, M.; Tian, B.; Zhang, J. Improving the visible light photocatalytic activity of nano-sized titanium dioxide via the synergistic effects between sulfur doping and sulfation. *Appl. Catal. B Environ.* **2012**, *115*, 253–260. [CrossRef]
162. Bakar, S.A.; Ribeiro, C. An insight toward the photocatalytic activity of S doped 1-D TiO_2 nanorods prepared via novel route: As promising platform for environmental leap. *J. Mol. Catal. A Chem.* **2016**, *412*, 78–92. [CrossRef]
163. Yan, X.; Yuan, K.; Lu, N.; Xu, H.; Zhang, S.; Takeuchi, N.; Kobayashi, H.; Li, R. The interplay of sulfur doping and surface hydroxyl in band gap engineering: Mesoporous sulfur-doped TiO_2 coupled with magnetite as a recyclable, efficient, visible light active photocatalyst for water purification. *Appl. Catal. B Environ.* **2017**, *218*, 20–23. [CrossRef]
164. Lv, Y.; Yuan, K.; Lu, N.; Xu, H.; Zhang, S.; Takeuchi, N.; Li, R. P-doped TiO_2 nanoparticles film coated on ground glass substrate and the repeated photodegradation of dye under solar light irradiation. *Appl. Surf. Sci.* **2011**, *257*, 5715–5719. [CrossRef]
165. Wu, J.; Zhang, Y.; Zhou, J.; Wang, K.; Zheng, Y.Z.; Tao, X. Uniformly assembling n-type metal oxide nanostructures (TiO_2 nanoparticles and SnO_2 nanowires) onto P doped g-C_3N_4 nanosheets for efficient photocatalytic water splitting. *Appl. Catal. B Environ.* **2020**, *278*, 119301. [CrossRef]
166. Zhang, G.; Ji, S.; Zhang, Y.; Wei, Y. Facile synthesis of pn heterojunction of phosphorus doped TiO_2 and BiOI with enhanced visible-light photocatalytic activity. *Solid State Commun.* **2017**, *259*, 34–39. [CrossRef]
167. Gopal, N.O.; Lo, H.H.; Ke, T.F.; Lee, C.H.; Chou, C.C.; Wu, J.D.; Ke, S.C. Visible light active phosphorus-doped TiO_2 nanoparticles: An EPR evidence for the enhanced charge separation. *J. Phys. Chem. C* **2012**, *116*, 16191–16197. [CrossRef]
168. Zhu, Y.; Li, J.; Dong, C.L.; Ren, J.; Huang, Y.C.; Zhao, D.; Yang, D. Red phosphorus decorated and doped TiO_2 nanofibers for efficient photocatalytic hydrogen evolution from pure water. *Appl. Catal. B Environ.* **2019**, *255*, 117764. [CrossRef]
169. Peng, Y.; He, J.; Liu, Q.; Sun, Z.; Yan, W.; Pan, Z.; Wei, S. Impurity concentration dependence of optical absorption for phosphorus-doped anatase TiO_2. *J. Phys. Chem. C* **2011**, *115*, 8184–8188. [CrossRef]
170. Olhero, S.M.; Ganesh, I.; Torres, P.M.; Ferreira, J.M. Surface passivation of $MgAl_2O_4$ spinel powder by chemisorbing H_3PO_4 for easy aqueous processing. *Langmuir* **2008**, *24*, 9525–9530. [CrossRef] [PubMed]

171. Mendiola-Alvarez, S.Y.; Hernández-Ramírez, A.; Guzmán-Mar, J.L.; Maya-Treviño, M.L.; Caballero-Quintero, A.; Hinojosa-Reyes, L. A novel P-doped Fe_2O_3-TiO_2 mixed oxide: Synthesis, characterization and photocatalytic activity under visible radiation. *Catal. Today.* **2019**, *328*, 91–98. [CrossRef]
172. Xia, Y.; Jiang, Y.; Li, F.; Xia, M.; Xue, B.; Li, Y. Effect of calcined atmosphere on the photocatalytic activity of P-doped TiO_2. *Appl. Surf. Sci.* **2014**, *289*, 306–315. [CrossRef]
173. Li, F.; Jiang, Y.; Xia, M.; Sun, M.; Xue, B.; Liu, D.; Zhang, X. Effect of the P/Ti ratio on the visible-light photocatalytic activity of P-doped TiO_2. *J. Phys. Chem. C* **2009**, *113*, 18134–18141. [CrossRef]
174. Valentin, C.; Pacchioni, G. Trends in non-metal doping of anatase TiO_2: B, C, N and F. *Catal. Today* **2013**, *206*, 12–18. [CrossRef]
175. Dozzi, M.V.; Selli, E. Doping TiO_2 with p-block elements: Effects on photocatalytic activity. *J. Photochem. Photobiol. C Photochem. Rev.* **2013**, *14*, 13–28. [CrossRef]
176. Kuo, C.-Y.; Jheng, H.-K.; Syu, S.-E. Effect of non-metal doping on the photocatalytic activity of titanium dioxide on the photodegradation of aqueous bisphenol A. *Environ. Technol.* **2021**, *42*, 1603–1611. [CrossRef]
177. Zheng, J.; Liu, Z.; Liu, X.; Yan, X.; Li, D.; Chu, W. Facile hydrothermal synthesis and characteristics of B-doped TiO_2 hybrid hollow microspheres with higher photo-catalytic activity. *J. Alloys Compd.* **2011**, *509*, 3771–3776. [CrossRef]
178. Bessegato, G.G.; Cardoso, J.C.; Zanoni, M.V.B. Enhanced photoelectrocatalytic degradation of an acid dye with boron-doped TiO_2 nanotube anodes. *Catal. Today* **2015**, *240*, 100–106. [CrossRef]
179. Yadav, V.; Verma, P.; Sharma, H.; Tripathy, S.; Saini, V.K. Photodegradation of 4-nitrophenol over B-doped TiO_2 nanostructure: Effect of dopant concentration, kinetics, and mechanism. *Environ. Sci. Pollut. Res.* **2020**, *27*, 10966–10980. [CrossRef]
180. Gao, Q.; Si, F.; Zhang, S.; Fang, Y.; Chen, X.; Yang, S. Hydrogenated F-doped TiO_2 for photocatalytic hydrogen evolution and pollutant degradation. *Int. J. Hydrogen Energy* **2019**, *44*, 8011–8019. [CrossRef]
181. Filippatos, P.-P.; Soultati, A.; Kelaidis, N.; Petaroudis, C.; Alivisatou, A.A.; Drivas, C.; Chroneos, A. Preparation of hydrogen, fluorine and chlorine doped and co-doped titanium dioxide photocatalysts: A theoretical and experimental approach. *Sci. Rep.* **2021**, *11*, 5700. [CrossRef]
182. Samsudin, E.M.; Hamid, S.B.A. Effect of band gap engineering in anionic-doped TiO_2 photocatalyst. *Appl. Surf. Sci.* **2017**, *391*, 326–336. [CrossRef]
183. Yu, W.; Liu, X.; Pan, L.; Li, J.; Liu, J.; Zhang, J.; Li, P.L.; Chen, C.; Sun, Z. Enhanced visible light photocatalytic degradation of methylene blue by F-doped TiO_2. *Appl. Surf. Sci.* **2014**, *319*, 107–112. [CrossRef]
184. Wang, X.-K.; Wang, C.; Jiang, W.Q.; Guo, W.L.; Wang, J.G. Sonochemical synthesis and characterization of Cl-doped TiO_2 and its application in the photodegradation of phthalate ester under visible light irradiation. *Chem. Eng. J.* **2012**, *189*, 288–294. [CrossRef]
185. Long, M.; Cai, W.; Chen, H.; Xu, J. Preparation, characterization and photocatalytic activity of visible light driven chlorine-doped TiO_2. *Front. Chem. China* **2007**, *2*, 278–282. [CrossRef]
186. Wang, Q.; Zhu, S.; Liang, Y.; Cui, Z.; Yang, X.; Liang, C.; Inoue, A. Synthesis of Br-doped TiO_2 hollow spheres with enhanced photocatalytic activity. *J. Nanoparticle Res.* **2017**, *19*, 72. [CrossRef]
187. Shen, Y.; Xiong, T.; Du, H.; Jin, H.; Shang, J.; Yang, K. Investigation of Br–N Co-doped TiO_2 photocatalysts: Preparation and photocatalytic activities under visible light. *J. Sol-Gel Sci. Technol.* **2009**, *52*, 41–48. [CrossRef]
188. Luo, H.; Takata, T.; Lee, Y.; Zhao, J.; Domen, K.; Yan, Y. Photocatalytic activity enhancing for titanium dioxide by co-doping with bromine and chlorine. *Chem. Mater.* **2004**, *16*, 846–849. [CrossRef]
189. Barkul, R.P.; Patil, M.K.; Patil, S.M.; Shevale, V.B.; Delekar, S.D. Sunlight-assisted photocatalytic degradation of textile effluent and Rhodamine B by using iodine doped TiO_2 nanoparticles. *J. Photochem. Photobiol. A Chem.* **2017**, *349*, 138–147. [CrossRef]
190. Gai, H.; Wang, H.; Liu, L.; Feng, B.; Xiao, M.; Tang, Y.; Qu, X.; Song, H.; Huang, T. Potassium and iodide codoped mesoporous titanium dioxide for enhancing photocatalytic degradation of phenolic compounds. *Chem. Phys. Lett.* **2021**, *767*, 138367. [CrossRef]
191. Van Viet, P.; Huy, T.H.; Sang, T.T.; Nguyet, H.M.; Thi, C.M. One-pot hydrothermal synthesis of Si doped TiO_2 nanotubes from commercial material sources for visible light-driven photocatalytic activity. *Mater. Res. Express* **2019**, *6*, 055006. [CrossRef]
192. Kim, M.G.; Kang, J.M.; Lee, J.E.; Kim, K.S.; Kim, K.H.; Cho, M.; Lee, S.G. Effects of calcination temperature on the phase composition, photocatalytic degradation, and virucidal activities of TiO_2 nanoparticles. *ACS Omega* **2021**, *6*, 10668–10678. [CrossRef]
193. Gaya, U.I.; Abdullah, A.H. Heterogeneous photocatalytic degradation of organic contaminants over titanium dioxide: A review of fundamentals, progress and problems. *J. Photochem. Photobiol. C Photochem. Rev.* **2008**, *9*, 1–12. [CrossRef]
194. Guettaï, N.; Amar, H.A. Photocatalytic oxidation of methyl orange in presence of titanium dioxide in aqueous suspension. Part I: Parametric study. *Desalination* **2005**, *185*, 427–437. [CrossRef]
195. Kinsinger, N.M.; Dudchenko, A.; Wong, A.; Kisailus, D. Synergistic effect of pH and phase in a nanocrystalline titania photocatalyst. *ACS Appl. Mater. Interfaces* **2013**, *5*, 6247–6254. [CrossRef]
196. Sun, J.; Wang, X.; Sun, J.; Sun, R.; Sun, S.; Qiao, L. Photocatalytic degradation and kinetics of Orange G using nano-sized Sn (IV)/TiO_2/AC photocatalyst. *J. Mol. Catal. A Chem.* **2006**, *260*, 241–246. [CrossRef]
197. Sun, J.; Qiao, L.; Sun, S.; Wang, G. Photocatalytic degradation of Orange G on nitrogen-doped TiO_2 catalysts under visible light and sunlight irradiation. *J. Hazard. Mater.* **2008**, *155*, 312–319. [CrossRef]
198. Baran, W.; Makowski, A.; Wardas, W. The effect of UV radiation absorption of cationic and anionic dye solutions on their photocatalytic degradation in the presence TiO_2. *Dye. Pigment.* **2008**, *76*, 226–230. [CrossRef]

199. Nhu, V.T.T.; QuangMinh, D.; Duy, N.N.; QuocHien, N. Photocatalytic Degradation of Azo Dye (Methyl Red) In Water under Visible Light Using AgNi/TiO_2 Sythesized by γ Irradiation Method. *Int. J. Environ. Agric. Biotechnol. (IJEAB)* **2017**, *2*, 529–538.
200. Kovalev, I.S. Stealth moths: The multi-plumed wings of the moth alucita hexadactyla may decrease the intensity of their echo to simulated bat echolocation cries. *Entomol. News* **2016**, *126*, 204–212. [CrossRef]
201. Ali, A.H. Study on the photocatalytic degradation of indigo carmine dye by TiO_2 photocatalyst. *J. Kerbala Univ.* **2013**, *11*, 145–153.
202. Viswanathan, B. Photocatalytic degradation of dyes: An overview. *Curr. Catal.* **2018**, *7*, 99–121. [CrossRef]
203. Đokić, V.R.; Vujović, J.; Marinković, A.; Petrović, R.; Janaćković, Đ.; Onjia, A.; Mijin, D. A study of the photocatalytic degradation of the textile dye CI Basic Yellow 28 in water using a P160 TiO_2-based catalyst. *J. Serb. Chem. Soc.* **2012**, *77*, 1747–1757. [CrossRef]
204. Mohabansi, N.; Patil, V.; Yenkie, N. A comparative study on photo degradation of methylene blue dye effluent by advanced oxidation process by using TiO_2/ZnO photo catalyst. *Rasayan J. Chem.* **2011**, *4*, 814–819.
205. Samsudin, E.M.; Goh, S.N.; Wu, T.Y.; Ling, T.T.; Hamid, S.A.; Juan, J.C. Evaluation on the photocatalytic degradation activity of reactive blue 4 using pure anatase nano-TiO_2. *Sains Malays.* **2015**, *44*, 1011–1019. [CrossRef]
206. Ram, C.; Pareek, R.K.; Singh, V. Photocatalytic degradation of textile dye by using titanium dioxide nanocatalyst. *Int. J. Theor. Appl. Sci.* **2012**, *4*, 82–88.
207. Meeti, M.; Sharma, T. Photo catalytic degradation of two commercial dyes in aqueous phase using photo catalyst TiO_2. *Adv. Appl. Sci. Res.* **2012**, *3*, 849–853.
208. Nagaraja, R.; Kottam, N.; Girija, C.R.; Nagabhushana, B.M. Photocatalytic degradation of Rhodamine B dye under UV/solar light using ZnO nanopowder synthesized by solution combustion route. *Powder Technol.* **2012**, *215*, 91–97. [CrossRef]
209. Choi, Y.; Koo, M.S.; Bokare, A.D.; Kim, D.H.; Bahnemann, D.W.; Choi, W. Sequential process combination of photocatalytic oxidation and dark reduction for the removal of organic pollutants and Cr (VI) using Ag/TiO_2. *Environ. Sci. Technol.* **2017**, *51*, 3973–3981. [CrossRef]
210. Guillard, C.; Disdier, J.; Monnet, C.; Dussaud, J.; Malato, S.; Blanco, J.; Maldonado, M.; Herrmann, J.-M. Solar efficiency of a new deposited titania photocatalyst: Chlorophenol, pesticide and dye removal applications. *Appl. Catal. B Environ.* **2003**, *46*, 319–332. [CrossRef]
211. Zhang, A.-Y.; Wang, W.K.; Pei, D.N.; Yu, H.Q. Degradation of refractory pollutants under solar light irradiation by a robust and self-protected ZnO/CdS/TiO_2 hybrid photocatalyst. *Water Res.* **2016**, *92*, 78–86. [CrossRef]
212. Azad, K.; Gajanan, P. Photodegradation of methyl orange in aqueous solution by the visible light active Co: La: TiO_2 nanocomposite. *Chem. Sci. J.* **2017**, *8*, 1000164.
213. Bhandari, S.; Vardia, J.; Malkani, R.K.; Ameta, S.C. Effect of transition metal ions on photocatalytic activity of ZnO in bleaching of some dyes. *Toxicol. Environ. Chem.* **2006**, *88*, 35–44. [CrossRef]
214. Kumar, A.; Pandey, G. A review on the factors affecting the photocatalytic degradation of hazardous materials. *Mater. Sci. Eng. Int. J.* **2017**, *1*, 106–114. [CrossRef]
215. Kumar, A.; Hitkari, G.; Gautam, M.; Singh, S.; Pandey, G. Synthesis, characterization and application of Cu-TiO_2 nanaocomposites in photodegradation of methyl red (MR). *Int. Adv. Res. J. Sci. Eng. Technol.* **2015**, *2*, 50–55. [CrossRef]
216. Hasanpour, M.; Hatami, M. Photocatalytic performance of aerogels for organic dyes removal from wastewaters: Review study. *J. Mol. Liq.* **2020**, *309*, 113094. [CrossRef]
217. Hinojosa–Reyes, M.; Camposeco–Solis, R.; Ruiz, F.; Rodríguez–González, V.; Moctezuma, E. Promotional effect of metal doping on nanostructured TiO_2 during the photocatalytic degradation of 4-chlorophenol and naproxen sodium as pollutants. *Mater. Sci. Semicond. Process.* **2019**, *100*, 130–139. [CrossRef]
218. Vorontsov, A.; Kabachkov, E.N.; Balikhin, I.L.; Kurkin, E.N.; Troitskii, V.N.; Smirniotis, P.G. Correlation of surface area with photocatalytic activity of TiO_2. *J. Adv. Oxid. Technol.* **2018**, *21*, 127–137. [CrossRef]
219. Ameen, S.; Seo, H.K.; Akhtar, M.S.; Shin, H.S. Novel graphene/polyaniline nanocomposites and its photocatalytic activity toward the degradation of rose Bengal dye. *Chem. Eng. J.* **2012**, *210*, 220–228. [CrossRef]
220. Cassano, A.E.; Alfano, O.M. Reaction engineering of suspended solid heterogeneous photocatalytic reactors. *Catal. Today* **2000**, *58*, 167–197. [CrossRef]
221. Muruganandham, M.; Swaminathan, M. TiO_2–UV photocatalytic oxidation of Reactive Yellow 14: Effect of operational parameters. *J. Hazard. Mater.* **2006**, *135*, 78–86. [CrossRef]
222. Elaziouti, A.; Ahmed, B. ZnO-assisted photocatalytic degradation of congo Red and benzopurpurine 4B in aqueous solution. *J. Chem. Eng. Process. Technol.* **2011**, *2*, 1000106.
223. Rafiq, A.; Ikram, M.; Ali, S.; Niaz, F.; Khan, M.; Khan, Q.; Maqbool, M. Photocatalytic degradation of dyes using semiconductor photocatalysts to clean industrial water pollution. *J. Ind. Eng. Chem.* **2021**, *97*, 111–128. [CrossRef]
224. Kaur, S.; Singh, V. TiO_2 mediated photocatalytic degradation studies of Reactive Red 198 by UV irradiation. *J. Hazard. Mater.* **2007**, *141*, 230–236. [CrossRef]
225. Shabir, M.; Yasin, M.; Hussain, M.; Shafiq, I.; Akhter, P.; Nizami, A.-S.; Jeon, B.-H.; Park, Y.-K. A review on recent advances in the treatment of dye-polluted wastewater. *J. Ind. Eng. Chem.* **2022**, *112*, 1–19. [CrossRef]
226. Muruganandham, M.; Swaminathan, M. Solar photocatalytic degradation of a reactive azo dye in TiO_2-suspension. *Solar Energy Mater. Sol. Cells* **2004**, *81*, 439–457. [CrossRef]
227. Litter, M.; Navio, J.A. Photocatalytic properties of iron-doped titania semiconductors. *J. Photochem. Photobiol. A Chem.* **1996**, *98*, 171–181. [CrossRef]

228. Leung, D.Y.; Fu, X.; Wang, C.; Ni, M.; Leung, M.K.; Wang, X.; Fu, X. Hydrogen production over titania-based photocatalysts. *ChemSusChem* **2010**, *3*, 681–694. [CrossRef] [PubMed]
229. Ma, T.; Akiyama, M.; Abe, E.; Imai, I. High-efficiency dye-sensitized solar cell based on a nitrogen-doped nanostructured titania electrode. *Nano Lett.* **2005**, *5*, 2543–2547. [CrossRef] [PubMed]
230. Mahmoud, M.; Ismail, A.A.; Sanad, M. Developing a cost-effective synthesis of active iron oxide doped titania photocatalysts loaded with palladium, platinum or silver nanoparticles. *Chem. Eng. J.* **2012**, *187*, 96–103. [CrossRef]
231. Han, X.; Kuang, Q.; Jin, M.; Xie, Z.; Zheng, L. Synthesis of titania nanosheets with a high percentage of exposed (001) facets and related photocatalytic properties. *J. Am. Chem. Soc.* **2009**, *131*, 3152–3153. [CrossRef]
232. Ikem, V.O.; Menner, A.; Bismarck, A. High-porosity macroporous polymers sythesized from titania-particle-stabilized medium and high internal phase emulsions. *Langmuir* **2010**, *26*, 8836–8841. [CrossRef]
233. Bartl, M.H.; Boettcher, S.W.; Frindell, K.L.; Stucky, G.D. 3-D molecular assembly of function in titania-based composite material systems. *Acc. Chem. Res.* **2005**, *38*, 263–271. [CrossRef]
234. Lindstrom, H.; Wootton, R.; Iles, A. High surface area titania photocatalytic microfluidic reactors. *AICHE J.* **2007**, *53*, 695–702. [CrossRef]
235. Peiris, S.; de Silva, H.B.; Ranasinghe, K.N.; Bandara, S.V.; Perera, I.R. Recent development and future prospects of TiO_2 photocatalysis. *J. Chin. Chem. Soc.* **2021**, *68*, 738–769. [CrossRef]